Hot Stamping of Manganese Boron Steel
(Technology Review and Preliminary Finite Element Simulations)

THESIS

Presented in Partial Fulfillment of the Requirements for the Degree Master of Science in the Graduate School of The Ohio State University

By

Ambikapathy Naganathan

Graduate Program in Mechanical Engineering

The Ohio State University

2010

Master's Examination Committee:

Professor Taylan Altan, Advisor

Professor Gary Kinzel

Abstract

The simulation of hot stamping is rather complex and challenging, and requires information about properties of die and sheet materials, heat transfer, and friction between the deforming material and the dies. A large number of researchers use different commercial codes , such as LS-Dyna, Pamstamp, Autoform, and DEFORM to conduct hot stamping simulations with various levels of success. In this study DEFORM, a commercial code widely used for the analysis of hot, cold and warm forging operations and die design has been used. This code can consider elastic and plastic deformations of the sheet material, friction, heat transfer and elastic deflections of the dies. Two part geometries have been analyzed, using information provided in the literature as well as that obtained from various companies that produce hot stamped parts. The results indicate that it is possible to predict the deformation and temperatures in the part and in the dies by considering the variation of interface heat transfer in function of interface pressure. Using this approach it is also possible to optimize the design of cooling channels in the dies. It appears that the approach, used in this study, is quite promising for use in industrial environment to optimize die and process design for hot stamping.

Dedication

This document is dedicated to my family

Acknowledgments

I am sincerely thankful to my advisor, Dr. Taylan Altan for his valuable support and guidance for this work. I am grateful to the sponsors, IMRA America Inc and POSCO for conducting this research.

I am also thankful to Dr.Choi, Adam, Luis, Deepak and all my colleagues at ERC/NSM for their valuable support at tough times.

Vita

2004	B.E. Mechanical Engineering, College of Engineering, Guindy, India
2004-2008	Lead Mechanical Engineer, Boiler and Heaters group, Thermax Limited, India
2010	Intern, Material Modeling Group, ANSYS Inc.,
2008-Present	Graduate Research Associate, Department of Mechanical Engineering, The Ohio State University

Fields of Study

Major Field: Mechanical Engineering

Table of Contents

List of Tables

List of Figures

CHAPTER 1.INTRODUCTION

In automotive industry, to improve vehicle safety and reduce fuel consumption, manufacturing of light weight body parts from Manganese Boron steel (22MnB5) is rapidly increasing. Forming of Ultra high strength steel at room temperature is limited by low formability and considerable spring back. Therefore, hot stamping is accepted as a viable alternative solution and widely used, Figure 1.1. "Hot stamping is a non isothermal forming process for sheet metals; where forming and quenching take place in the same forming step"[MERK06b]. This process takes advantage of low flow stress of boron alloyed steel (22MnB5) in austenitic phase at elevated temperature and allows the manufacturing of parts with ultra high strength, minimum spring back and reduced sheet thickness.

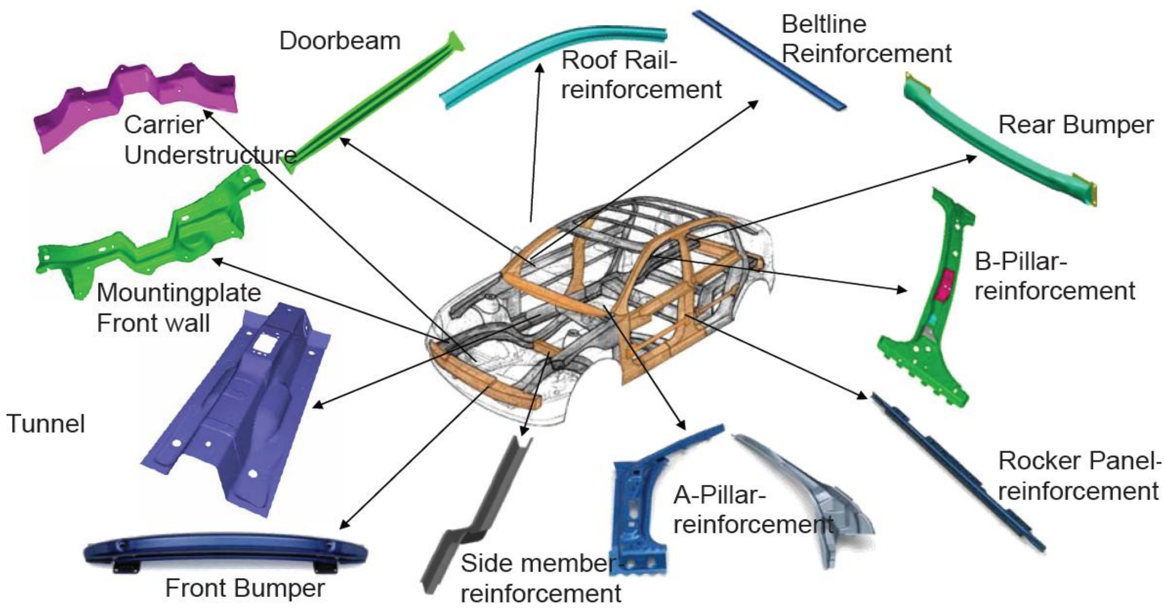

Figure 1.1 Components manufactured using hot stamping [BRYAN07]

Hot stamping was developed and patented in 1977 by a Swedish company (Plannja), which used the process for saw blades and lawn mover blades [KARB09]. In 1984, Saab Automobile AB was the first vehicle manufacturer who adopted a hardened boron steel component for the Saab 9000[BERG08a].The number of produced parts increased from 3 million parts/year in 1987 to 8 million parts/year in 1997 which went up to approximately 107 million parts/year in 2007[ASPA08].

There are two different methods of hot stamping: direct and indirect.

1.1 Direct method

In the direct method(Figure 1.2), the 22MnB5 blanks are austenitised at temperatures between 900 and 950°C for 4 to 10 minutes inside a continuous feed furnace and subsequently transferred to an internally cooled die set via a transfer unit. The transfer usually takes less than 3 seconds. At high temperature (650 to 850°C), the material has high formability and complex shapes can be formed in a single stroke. The blanks are stamped and cooled down under pressure for a specific amount of time according to the sheet thickness after drawing depth is reached. During this period the formed part is quenched in the closed die set that is internally cooled by water circulation at a cooling rate of 50 to 100°C/s, completing the quenching (martensitic transformation) process. The total cycle time for transferring, stamping, and cooling in the die is 15 to 25 seconds. The part leaves the hot stamping line at about 150°C and with high mechanical properties of 1400 to 1600 MPa and a yield strength between 1000 and 1200MPa.Because of the high strength of final part, operations like final trimming and piercing are difficult to achieve.

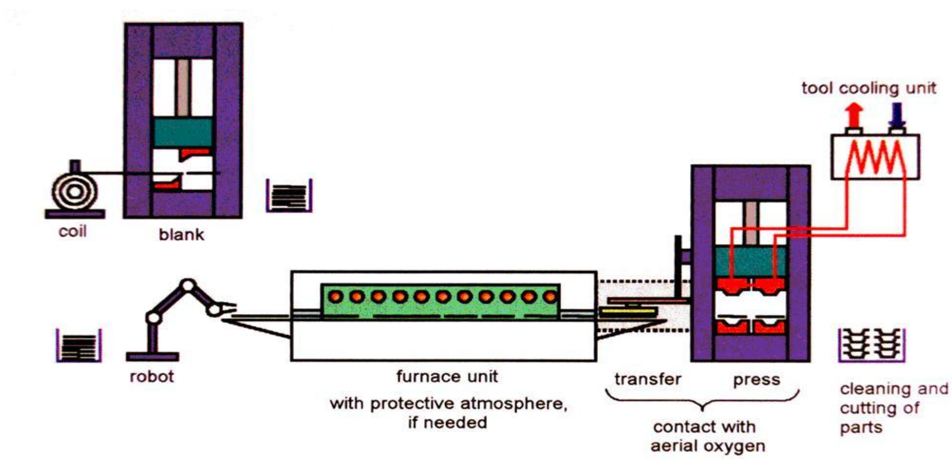

Figure 1.2 Direct method of hot stamping [ENGE06]

1.2 Indirect method

Unlike the direct process, indirect hot stamping (Figure 1.3), provides a part to be drawn, unheated, to about 90 to 95 percent of its final shape in a conventional die, followed by a partial trimming operation, depending on edge tolerance. Then the preforms are heated in a continuous furnace and quenched in the die. The reason for the additional step is to extend the forming limits for very complex shapes by hot forming and quenching the cold formed parts.

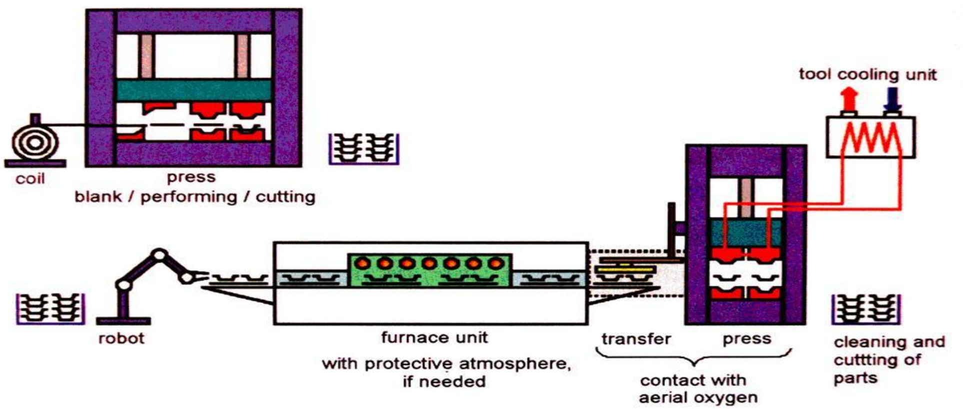

Figure 1.3 Indirect method of hot stamping [ENGE06]

CHAPTER 2. OBJECTIVE AND APPROACH

2.1 Objective

The objective of this work is to conduct a study on hot stamping technology, gather information for conducting successful finite element simulation of entire hot stamping process and run preliminary simulations using FE code DEFORM.

2.2 Approach

A state of the art review has been conducted and information were collected on the following topics

Material properties of 22MnB5

- Flow stress data
- Coefficient of friction and lubrication
- Heat transfer coefficient
- Formability and forming limit diagrams
- Phase transformation test
- Anisotropy coefficient
- Elastic properties

Tools for hot stamping

Blank heating methods

Coatings for oxidation prevention

Example finite element simulations

This review was followed by preliminary simulation of hot stamping experiments conducted at Lulea University of Technology, Sweden and Benchmark problem-3 proposed by AUDI in Numisheet-2008 conference.

CHAPTER 3. TECHNOLOGY REVIEW

3.1 Mechanical and tribological properties of 22MnB5

3.1.1 Continuous Cooling Transformation Curve

The continuous cooling transformation curve (CCT) illustrates the micro structural evolution of a particular material depending on the cooling rate. In order to reach tensile strength up to 1600 MPa of the final part, a complete transformation of the austenitic to martensitic microstructure is required. Therefore, cooling rates faster than 27K/s in the part have to be achieved to avoid bainitic or even ferritic- perlitic transformation, as shown in Figure 3.1.

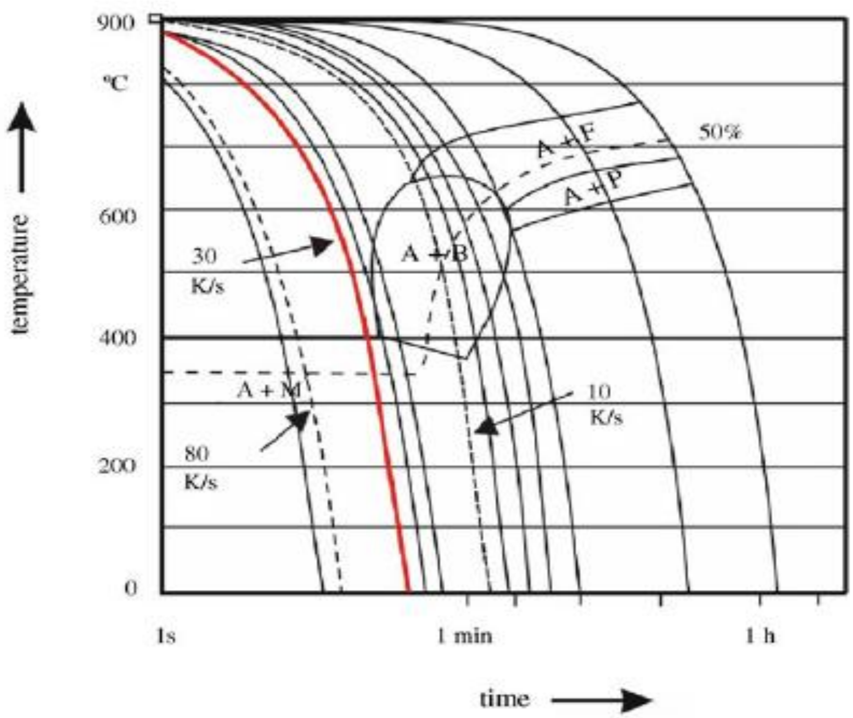

Figure 3.1 CCT diagram of 22MnB5 from Arcelor (A-Austenite, B-Bainite, F-Ferrite, P-Pearlite, M-Martensite) [MERK06b]

3.1.2 Chemical composition of 22MnB5

The addition of boron into the steel alloy lowers critical cooling rate and therefore extends the process window, Table 3.1.Furthermore, alloying boron reduces the carbon equivalent and therefore increases the weldability. Chrome and Manganese increase the tensile strength of the quenched material.

Table 3.1 Chemical composition of USIBOR 1500 (1.2mm thick), weight-% [BERG08]

Material	C	Mn	Si	Ni	Cr	Cu	S	P	Al	V	Ti	B
USIBOR	0.221	1.29	0.28	0.013	0.193	0.01	0.001	0.018	0.032	0.005	0.039	0.0038

3.1.3 Flow stress data for 22MnB5

Reliable FE simulation of hot stamping process requires accurate flow stress data. For 22MnB5 steel, flow stress data were obtained as a function of temperature, strain and strain rate using a modified Gleeble system (Figure 3.2) ([ERIK02], [MERK06a], [MERK06b], [TURE06]).

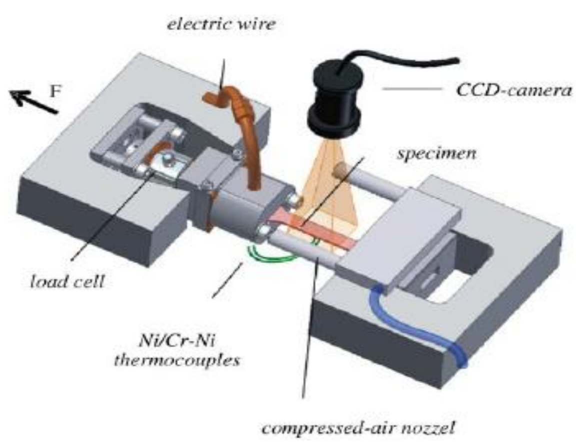

Figure 3.2 Modified Gleeble 1500 system [MERK06b]

The rolling direction does not have any influence on the flow stress data. Temperature has strong influence on the flow stress as given by the experimental values in Figure 3.3.

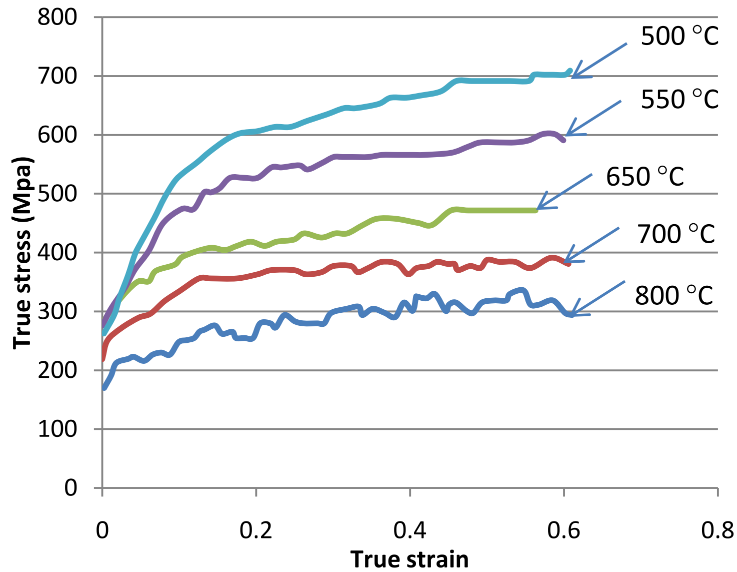

Figure 3.3 Influence of temperature on flow stress data, cooling rate=80K/s, strain rate=0.1s-1 [MERK06A]

With increase in temperature, there is a decrease in the flow stress values and the work hardening exponent. Furthermore, the curve shows an asymptotic trend around 700 to 800 C. This behavior is due to the temperature induced dynamic, micro structural recovery process balancing the strain hardening effect.

Increase in strain rate increases the flow stress level and strain hardening exponent, Figure 3.4. Increase in the strain hardening exponent is due to the short annihilation or recovery time available during the test.

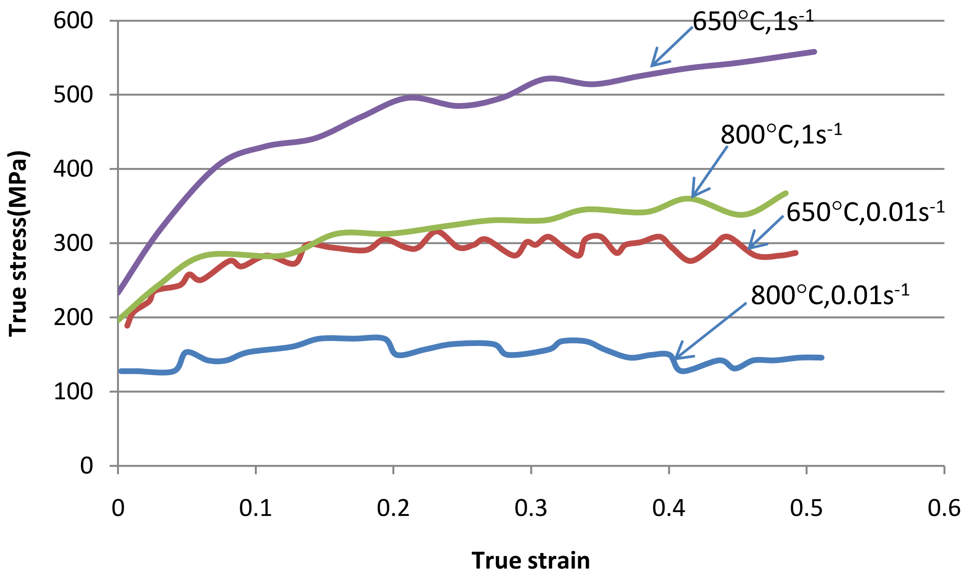

Figure 3.4 Influence of strain rate, cooling rate=80K/s [MERK06a]

At 500 C, lowest strain rate, 0.01 s-1 , leads to higher flow stress values as shown in the Figure 3.5.

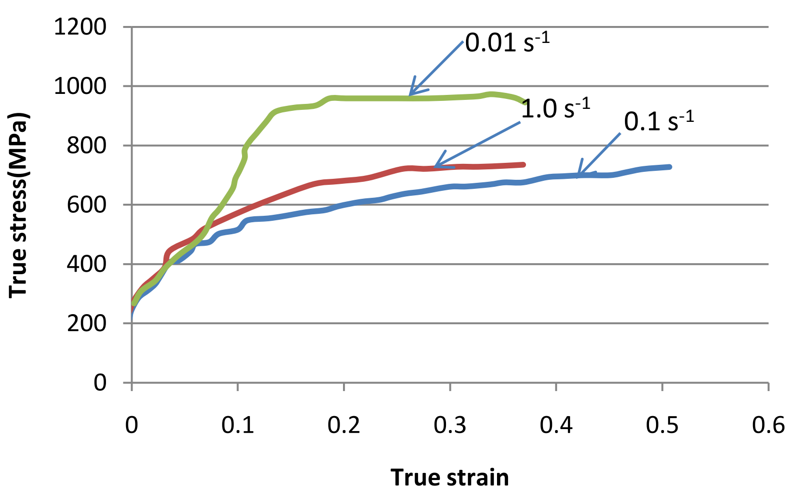

Figure 3.5 Influence of strain rate at 500 C, cooling rate=80K/s [MERK06a]

The reason for significant increase of flow stress at strain rate 0.01 s-1 is due to the sudden initiation of the micro structural transformation from austenite to bainite. For higher strain rates deformation takes place in the austenitic phase and the flow stress values show conventional behavior [MERK06a].

To study the effect of cooling rate, tests were conducted at air cooling rate of 15 K/s and a rapid cooling rate of 80 K/s and the results are shown in the Figure 3.6.

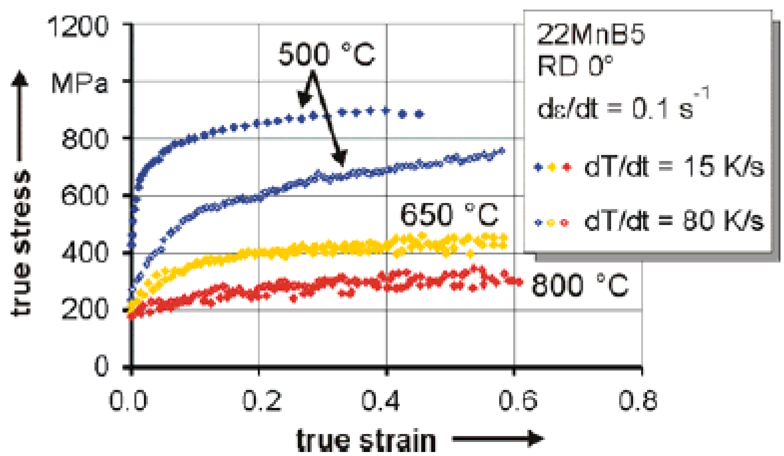

Figure 3.6 Influence of cooling rate [MERK06a]

At 650 and 800 C, the flow stress values have no effect on the cooling rate. At 500 C, bainite formation caused an increase of flow stress at lower cooling rate of 15 K/s.

3.1.4 Friction coefficient

The friction coefficient is an important parameter for calculating accurate material flow and heat transfer during hot stamping simulation. The friction coefficient under relevant conditions of hot stamping is calculated using a tribosimulator [YANA09] and modified cup drawing test [GEIG08]. Figure 3.7 represents the schematic of the testing machine used for determining friction in hot stamping [YANA09].

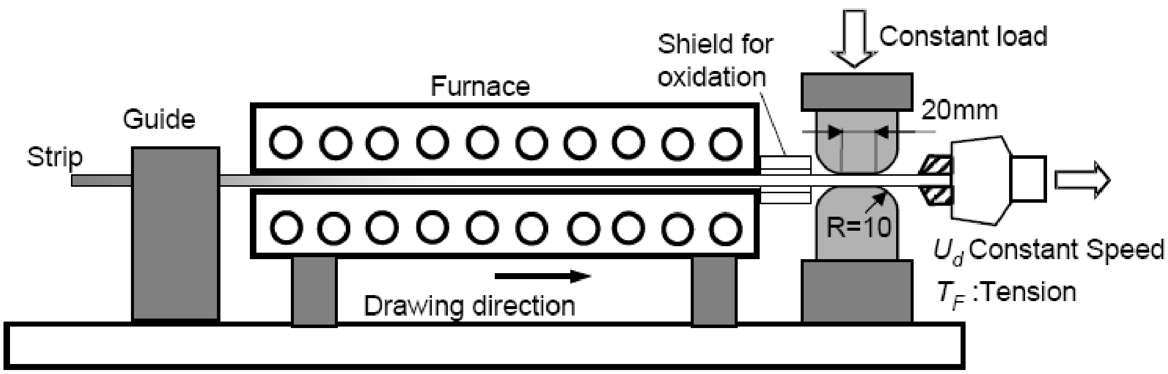

Figure 3.7 Schematic of testing machine used to determine friction in hot stamping [YANA09]

The 22MnB5 sheet material is heated in the infrared furnace to its austenitisation temperature under inert gas atmosphere of Ar. One end of the strip is clamped with the chuck of the tension device and it is pulled at constant speed. Once the heated zone of the strip reaches the entrance of the die, a constant compression load P is applied. The coefficient of friction, μ is calculated from constant compression load P and tension load TF using the equation

$$\mu=TF/2P \quad \text{……………………………………………….} (3.1)$$

The experiments were conducted under dry condition without lubricants.

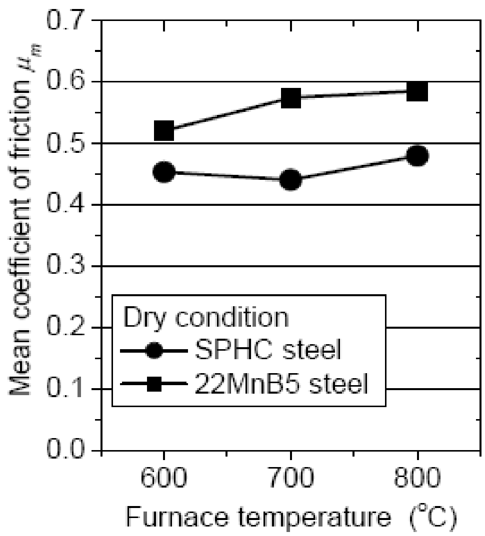

Figure 3.8 Effect of temperature on mean friction coefficients under dry conditions [YANA09]

Figure 3.8 shows, with an increase in the temperature, there is an increase in the friction coefficient for 22MnB5 steel and the effect is small for SPHC steel. This effect is due to the scale thickness generated during preheating. Figure 3.9 represents the schematic of the modified cup drawing test which is also suggested for determining the coefficient of friction [GEIG08].

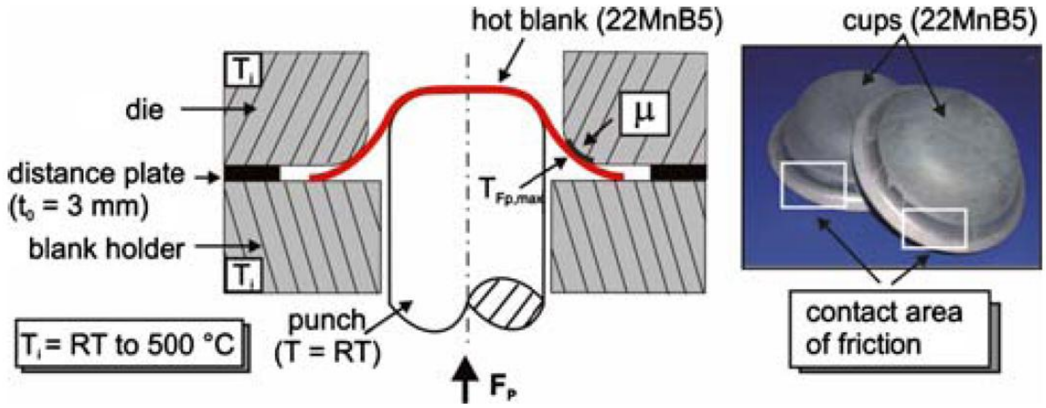

Figure 3.9 Schematic of the experimental setup of the cup deep drawing test (left) and two drawn cups at elevated temperatures [GEIG08]

The tool is connected to hydraulic press equipped with load cells for measuring the punch force, Fp and the blank holder force, FBH during the test. The sheet samples are heated in furnace .The tests were conducted without applying blank holder force in the flange area of the sheet to avoid unnecessary heat transfer. The tests were conducted with punch velocity (Vpunch) of 10mm/s. The temperature of the punch (Tpunch) was kept constant at room temperature (RT). Each parameter combination was tested at least 5 times (n=5).The coefficient of friction is calculated using the equation used to estimate the maximum deep drawing force by Siebel [SIEB55].

From Figure 3.10 and Figure 3.11, it is seen that the friction coefficient decreases with an increase in the temperature of the die and the blank holder. The significant temperature dependent plastic softening of the material 22MnB5 leads to reduced normal forces transferred from the bulk sheet material to the interacting surfaces at the die. This causes reduction in friction coefficient with increase in temperature.

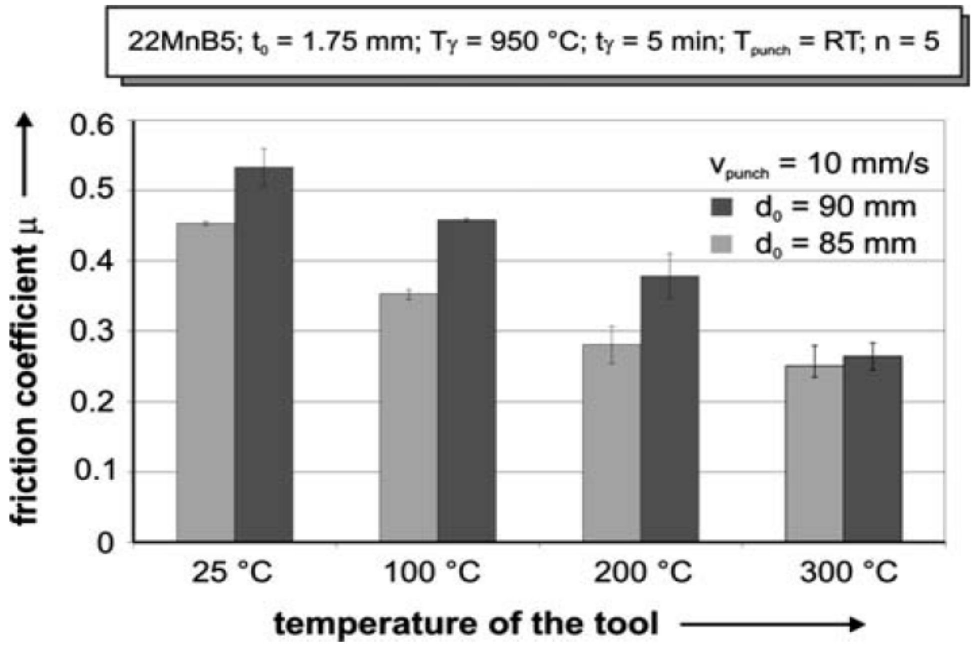

.

Figure 3.10 Evolution of friction coefficient μ with different tool temperature maintaining punch at room temperature for 22MnB5 sheet thickness t0= 1.75mm; austenitisation temperature T γ = 950°C; austenitisation time t γ=5 min; punch velocity vpunch = 10mm/s ,do=initial blank diameter [GEIG08]

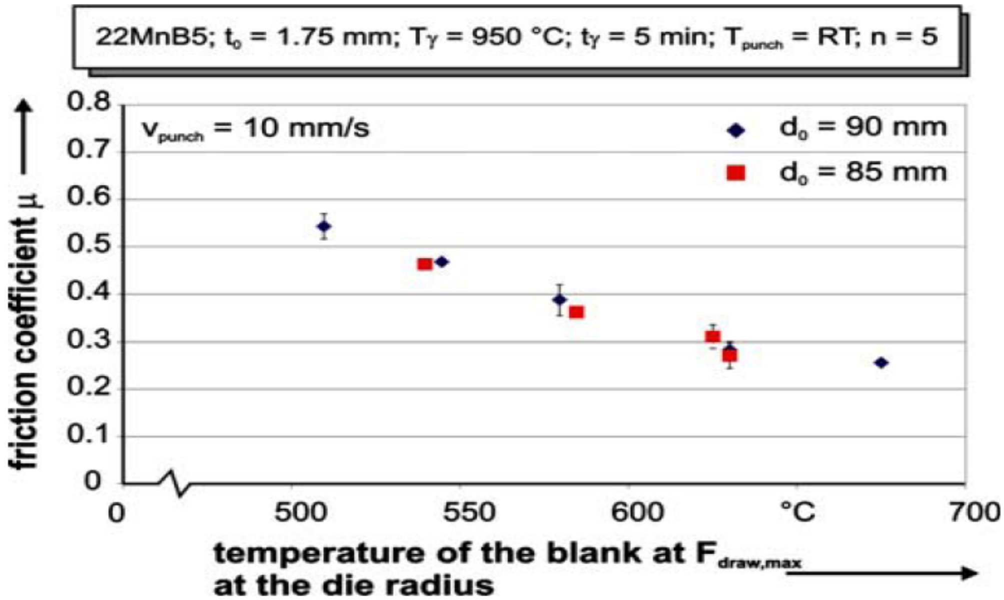

Figure 3.11 Friction coefficient μ as function of the blank temperature in the contact area at the die radius at the moment of the maximum drawing force for 22MnB5 sheet thickness t0= 1.75mm; austenitisation temperature T γ= 950°C; t γ=5 min; punch velocity vpunch = 10mm/s [GEIG08]

3.1.5 Heat transfer coefficient

The heat transfer between sheet material and die with integrated cooling channels determine the martensite formation and final part properties. The experimental setup for calculating the contact heat transfer coefficient between sheet materials and die is shown in Figure 3.12.

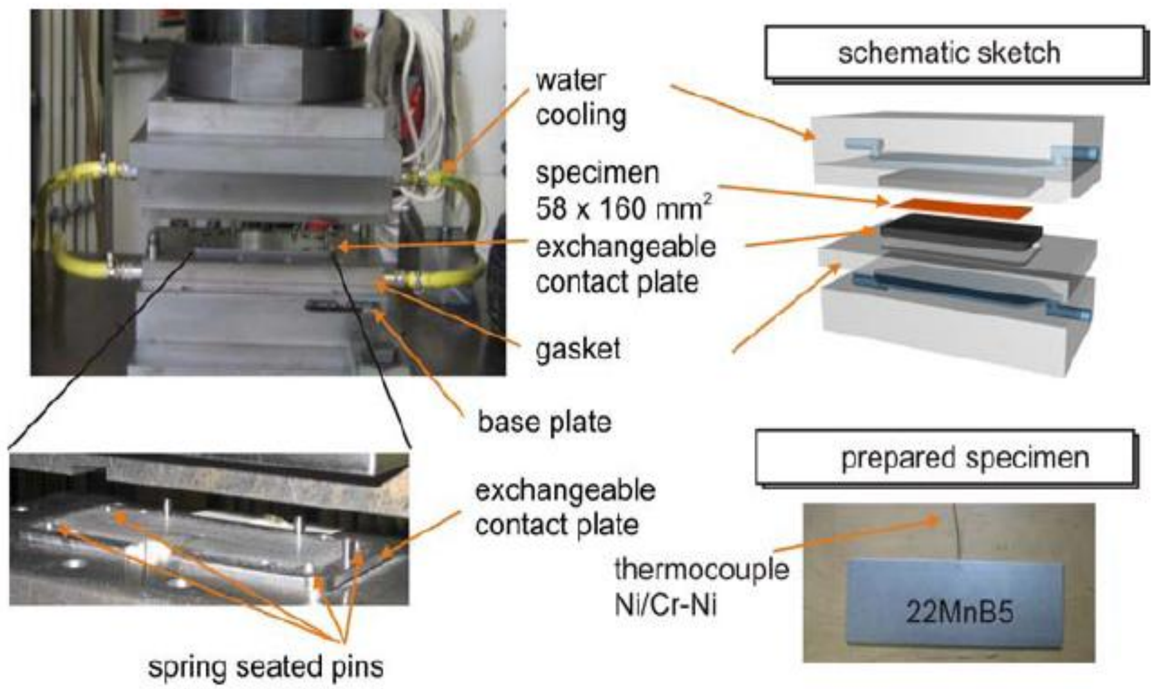

Figure 3.12 Experimental setup for finding heat transfer coefficient [MERK08a]

The setup contains two water cooled rectangular plates for quenching the specimen under pressure. The specimen is heated in a furnace to the austenitisation temperature of 850°C to 950°C and placed manually on four spring seated pins. With this experimental setup, the specimens can be loaded during quenching up to a pressure of 40 MPa. The heat transfer coefficient is calculated using Newton's cooling law given by the equation

$$T(t) = (T_0 - T_u) \cdot e^{-\alpha \cdot \frac{A}{cp} \cdot t} + T_u \quad \text{……………………………………………………(3.2)}$$

Where T0 and T(t) are initial and current temperature of the specimen during cooling experiment. Tu is the temperature of the contact plates. 't' is the time during the experiment. ‘A’ is the geometric contact area and ‘Cp’ is the heat capacity of the specimen.

The heat transfer coefficient α is calculated at a particular time ‘t’ from the above equation and the corresponding contact pressure is measured from the experiment.The contact pressure ranges from 0 to 40 MPa. The specimens were heated to the austenitisation temperature of 950°C for 5 minutes. The experiments were repeated for 5 specimens (n=5).The heat transfer coefficient increases as a function of pressure due to the increase in contact surface area and the results are given in the Figure 3.13.

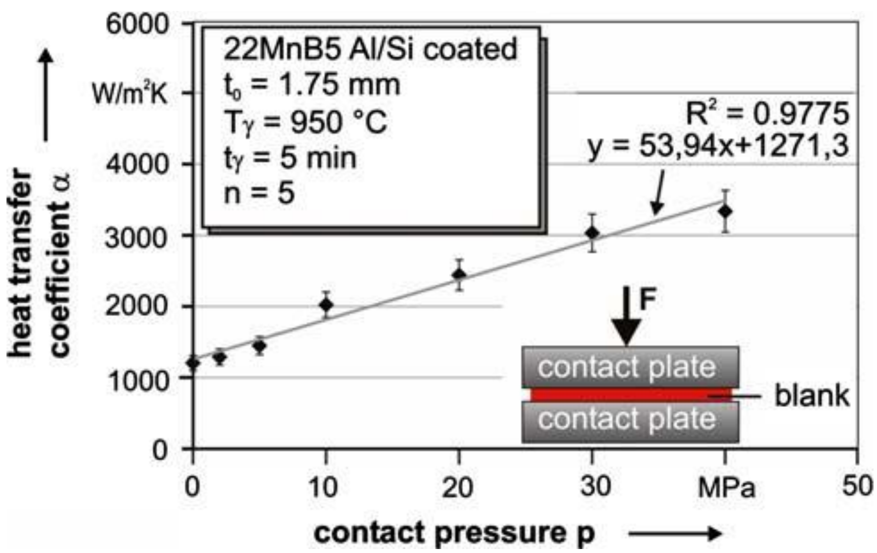

Figure 3.13 Heat transfer coefficient as a function of pressure for both sided metallic contact [GEIG08]

[LECH09] studied the variation of heat transfer coefficient as a function of contact distance between die and sheet surface. The results showed that the heat transfer coefficient between die and sheet material is almost constant (~100 W/m2K) till the contact distance reaches 0.5mm and the value increases steeply to 1200 W/m2K when the die touches the sheet material. The results are given in Figure 3.14.

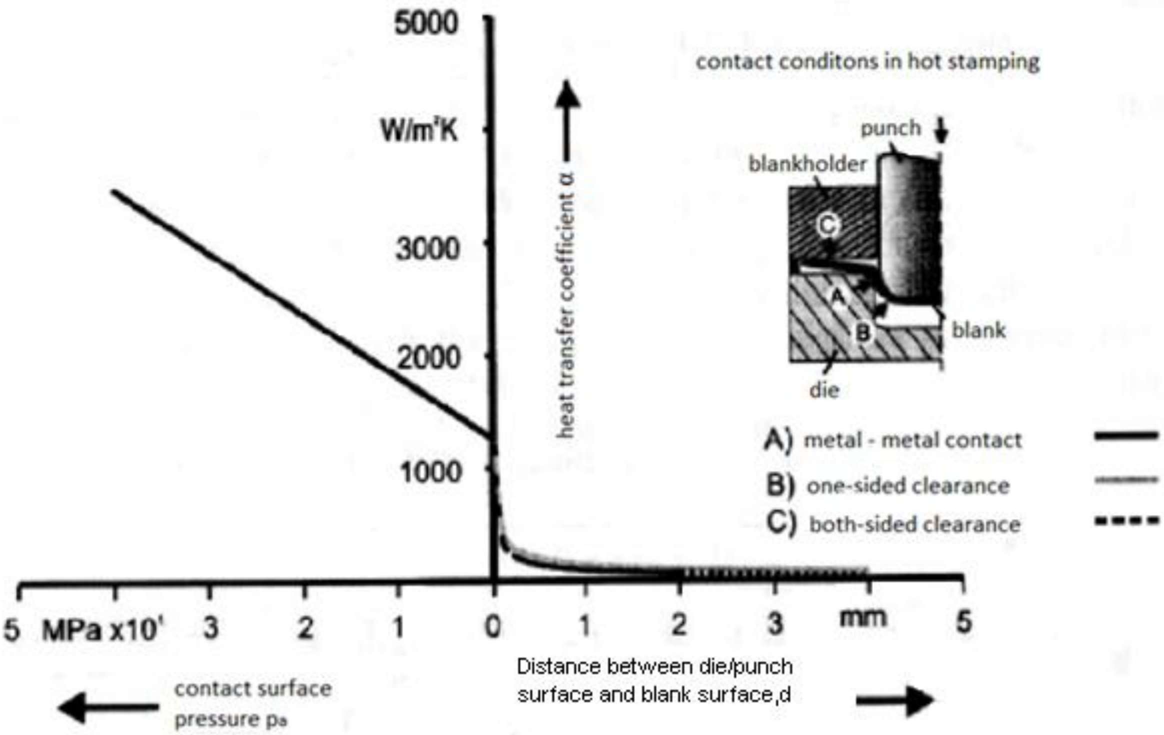

Figure 3.14 Contact heat transfer coefficient as a function of contact pressure and distance between tool and sheet material surface [LECH09]

3.2 Heating methods

In conventional hot stamping process, continuous furnaces are used whereas the blank is heated by radiation and convective flow of heat. The furnaces are heated with gas or electricity. The heating rate of the blanks is controlled by the speed of rollers or walking beams in the furnace. For 22MnB5 steel with Al-Si coating, a heating rate of 12K/s is recommended to avoid melting of Al-Si layer and to improve the diffusion of Fe into Al-Si layer. For complete austenitisation a dwell time of 145s is necessary at 1223K independent of the steel supplier and thickness of Al-Si coating for a sheet thickness of 1mm. With increase in the sheet thickness, the austenitisation time is also increasing; 165s for 1.5mm, 180s for 1.75mm, 240s for 2.5mm [KOLL09].

3.2.1 Conductive heating

During hot stamping process, the sheet is transferred from the furnace to the press. During this transfer, the sheet metal looses heat and also oxidizes. This may be avoided in conductive heating method by directly heating the sheets, set into the dies by means of electrical resistance.

In conduction heating method, the component is connected to a series of power source. Due to the electric resistance of the component the heat is generated proportional to the loss of power. This method can be used for partial heating of the sheet metal. In the field of sheet metal forming, conduction heating is currently used at laboratory level in material characterization experiments [KOLL09].

The resistance heating method is rapid enough to synchronize with a press during hot stamping process. Figure 3.15 shows the schematic of the resistance heating method developed by [MORI05].The sheet material is kept in between the dies and the electric current is passed through the electrodes. The time interval between end of the heating to the beginning of the forming process is 0.2s.A holding pressure of 7.4MPa was applied to maintain sufficient contact between the sheet and electrode. During the electrification process, the sheet is not in contact with die, blank holder and punch to avoid loss of heat.

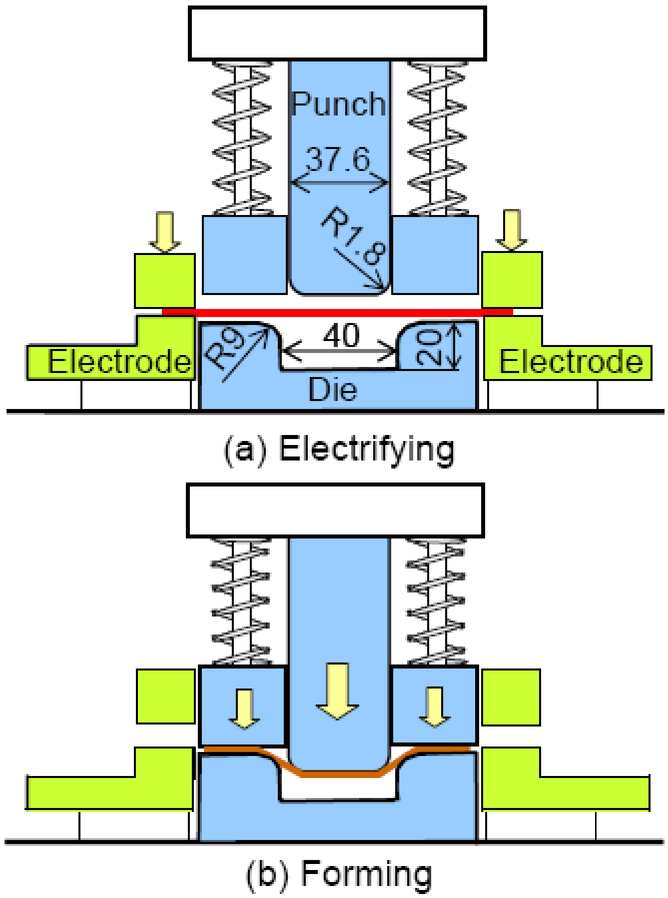

Figure 3.15 Hot stamping process using resistance heating [MORI05]

3.2.2 Induction heating

Similar to conduction heating method, induction heating is also used in laboratory level for hot stamping applications. It contains two major components; a high frequency generator and an induction coil (inductor).When an electricity conducting component enter the inductor, an electric current is induced in the component which generates heat. This eddy current depends on the operating frequency, electrical conductivity and the permeability of the material. The frequency of the generator determines the depth of heating. Low frequencies lead to a high penetration depth and high frequencies lead to low penetration depth.

There are three types of induction coils available; longitudinal field, cross field and face field inductors as shown in the Figure 3.16.

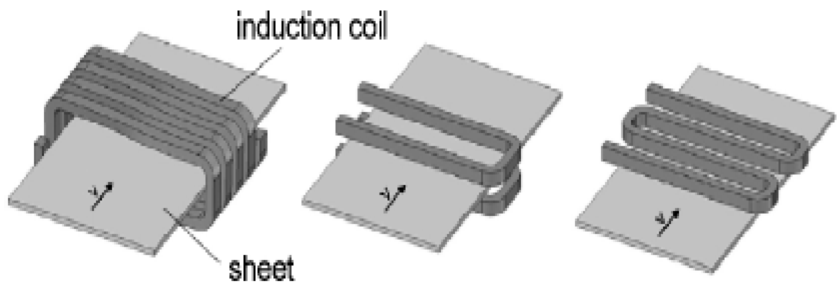

Figure 3.16 Principle design of longitudinal field, transverse field and face inductor [KOLL09]

The type of inductor determines the position of the magnetic field in reference to the work piece resulting in different efficiency. Heating steel sheets up to their Curie temperature in a longitudinal field inductor is characterized by an efficiency 93%.The Curie temperature for different steel grades ranges between 993K and 1018K.This method gives a homogeneous temperature distribution. For a further rise in temperature face inductor is necessary, changing the orientation of the magnetic field. In face inductor, the efficiency factor is 60% and the temperature distribution is not as homogeneous as longitudinal field inductor. Heating sheet metal from room temperature to 1223K with only a face inductor leads to a temperature deviation of 50K along the specimen. Thus it is recommended to use face induction as second heating step from Curie temperature to austenitisation temperature as shown in Figure 3.17. This leads to maximum temperature deviations of ±10K.

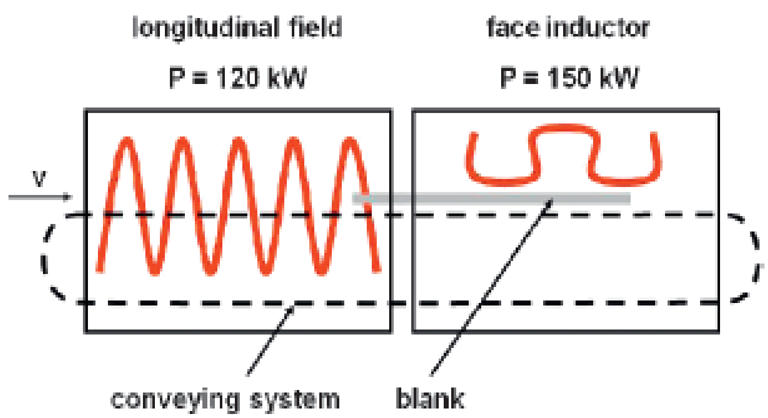

Figure 3.17 Fundamental principle of two-step induction heating device [KOLL09]

[KOLL09] used two step induction heating device (Figure 3.17) to heat 22MnB5 steel specimen. The system contains longitudinal field inductor with a maximum connected power of 120kW and a face inductor with a maximum connected power of 150kW. The transport of the blank is done with a chain drive fixed to the blank.

In the longitudinal field inductor, feed speed affects the heating rate. In the face inductor, the distance between sheet surface and induction coil is the governing parameter for achieving the required temperature.

3.3 Tools (Dies) for hot stamping

The complete tooling solution contains the tool steel, die design and construction, die coating, process parameters, and die maintenance [PAAR07].

3.3.1 Die design

Two main functions of the hot stamping die are forming the part and extracting the heat from the blank. The tool must be able to achieve a minimum cooling rate of 27 K/s to guarantee a complete martensitic transformation. Furthermore, the heat extraction capability of the die determines the productivity of the hot stamping line [PAAR07]. The die must absorb and evacuate an amount of energy up to 100 kW by means of integrated cooling devices [WILS06]. This results in high temperature gradients (up to 25K/mm) and induces high stresses in the surface layers. The total mechanical loading in the die is a combination of the stresses caused by temperature gradients and the direct mechanical loadings (forming and closing pressure) [PAAR07]. [WILS06] notes that hot stamping dies are usually designed to work without blank holder in order to minimize heat loss in the flange area during the forming operation.

Since the heat transfer coefficient depends on the contact pressure an excellent contact over the whole part is essential to avoid ―hot spots during quenching. This requires a precise tool design and a good surface condition. Three principles to improve the heat transfer in the tooling are using die material with higher heat conductivity, avoiding thermal barriers, and optimizing the cooling strategy [PAAR07].

In order to maintain the dimensional tolerances and the efficiency in heat transfer, desirable during hot stamping, the wear resistance of the tool material is an important issue [PAAR07]. [PAAR07] specifies the most typical failure mechanisms of hot stamping tools to be cracking, wear and sticking of the sheet coating on the die surface. [PAAR07] further explains that the cracks usually occur at the cooling channel and then grow to the die surface.

3.3.2 Tool steels

[WILS06] remarks that it is necessary to come to a compromise between good wear resistance over a wide temperature range and a good thermal conductivity. [WILS06] explains that an increasing percentage of alloying elements improves the hardness but affects the heat conductivity negatively. [PAAR07] states that most hot stamping dies are made of hot working steel (hardness > 44 HRC). Since the mechanical loads on the tool are not excessively high a tool material with strength above 1500 MPa prevents plastic tool deformation.

3.3.3 Optimization of locations of cooling channels in hot stamping dies

In the hot stamping process, the tool motion (time required to deform the part) requires relatively short time compared to quenching process. Optimization of the cooling system in the hot stamping tools will greatly reduce the cycle time, since cooling the part after the dies are closed is critical to achieve the desired cooling rate [HOFF07].

The following factors are identified to affect heat transfer between drawn part and die [STEI07].

(i) Heat transfer from the drawn part to the tool

-depends on surface scaling effects and gap between part and tool surface

(ii) Heat conductivity of the tool material

- depends on choice of tool material

(iii)Design of the cooling ducts

- defined by size location and distribution of the cooling ducts

(iv) Temperature and type of coolant.

-The temperature difference between coolant and tool affects the heat transfer

A method for optimizing the design of cooling channels was developed by Steinbeiss et al. [STEI07] at Institute of metal forming and Casting, Technische Universität München, Garching, Germany. The tests conducted and the results obtained by [STEI07] are summarized in the following sections.

The die arrangement and the test geometry of the blank and the drawn part for the optimization experiment are shown in Figure 3.18.In order to provide an effective cooling system, the four tool components punch, counterpunch, female die and blank holder are actively cooled with cooling ducts.

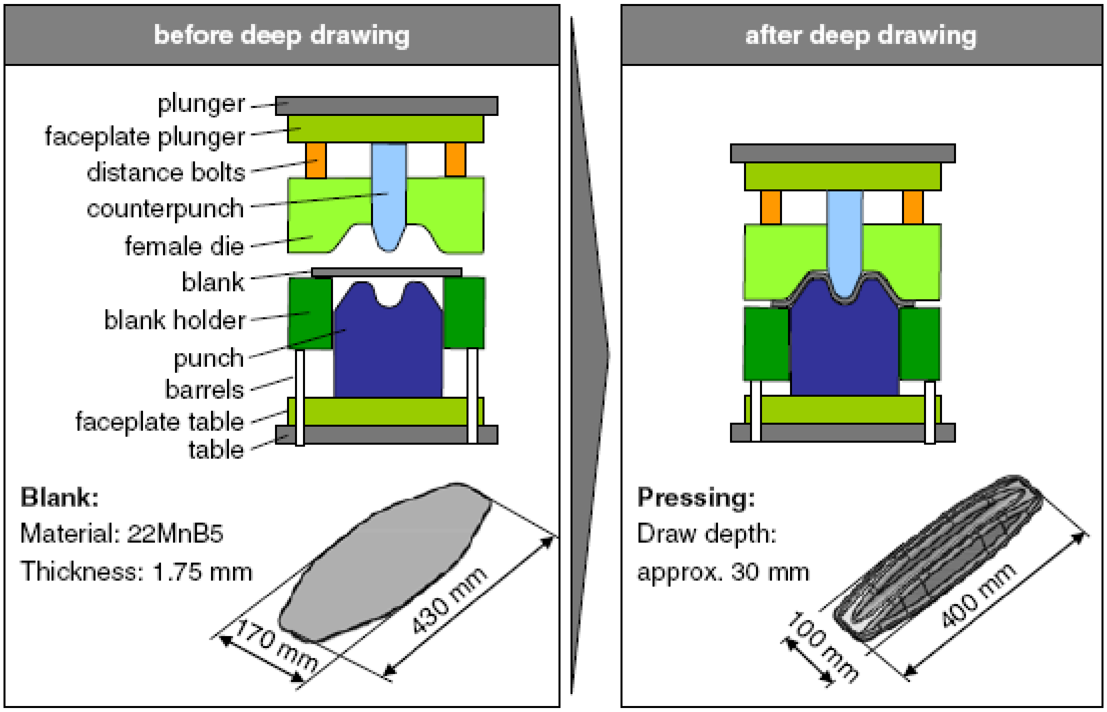

Figure 3.18 Test geometry and drawn part [STEI07]

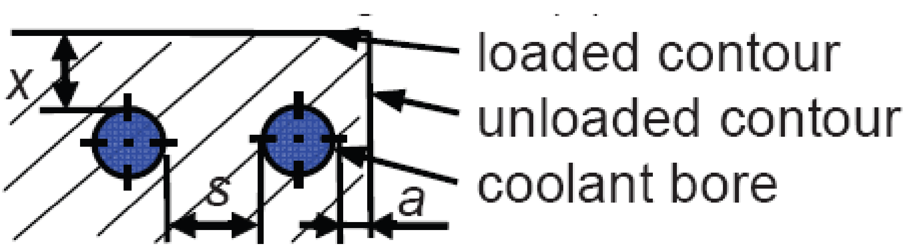

Figure 3.19 Schematic of tool surface [HOFF07]

Any tool surface can be divided into loaded and unloaded contours based on the subjected thermal and mechanical loading conditions. The constraints for the tool design are [HOFF07] (as seen in Figure 3.19)

(i) Minimum distance between loaded die surface (contour) and cooling duct (x)

(ii) Minimum distance between unloaded die surface (contour) and cooling duct (a)

(iii) Minimum distance between the cooling ducts(s)

(iv) Size of available sealing plugs which are used to divert the flow of coolants in the cooling duct

(v) Position of the cooling duct

As a first step in the tool design the above parameters are calculated based on expertise or results of preliminary FE calculations. The optimization is carried out using an evolutionary algorithm (EA) considering the criteria of cooling intensity of tool (cooling rate to be achieved) and uniform cooling. Evolutionary Algorithm (EA) was used to place the cooling channels optimally according to the given input and constraints. Figure 3.20 gives flow chart for the evolutionary algorithm.

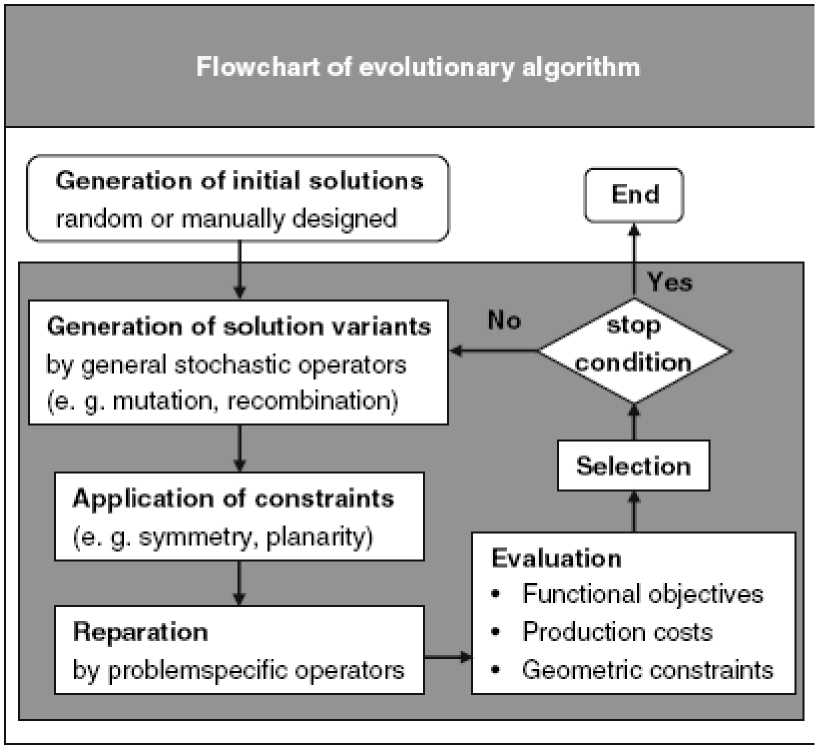

Figure 3.20 Flow chart of the evolutionary algorithm [STEI07]

Figure 3.21 gives an example of the optimized design of cooling system for a chosen drill hole diameter.

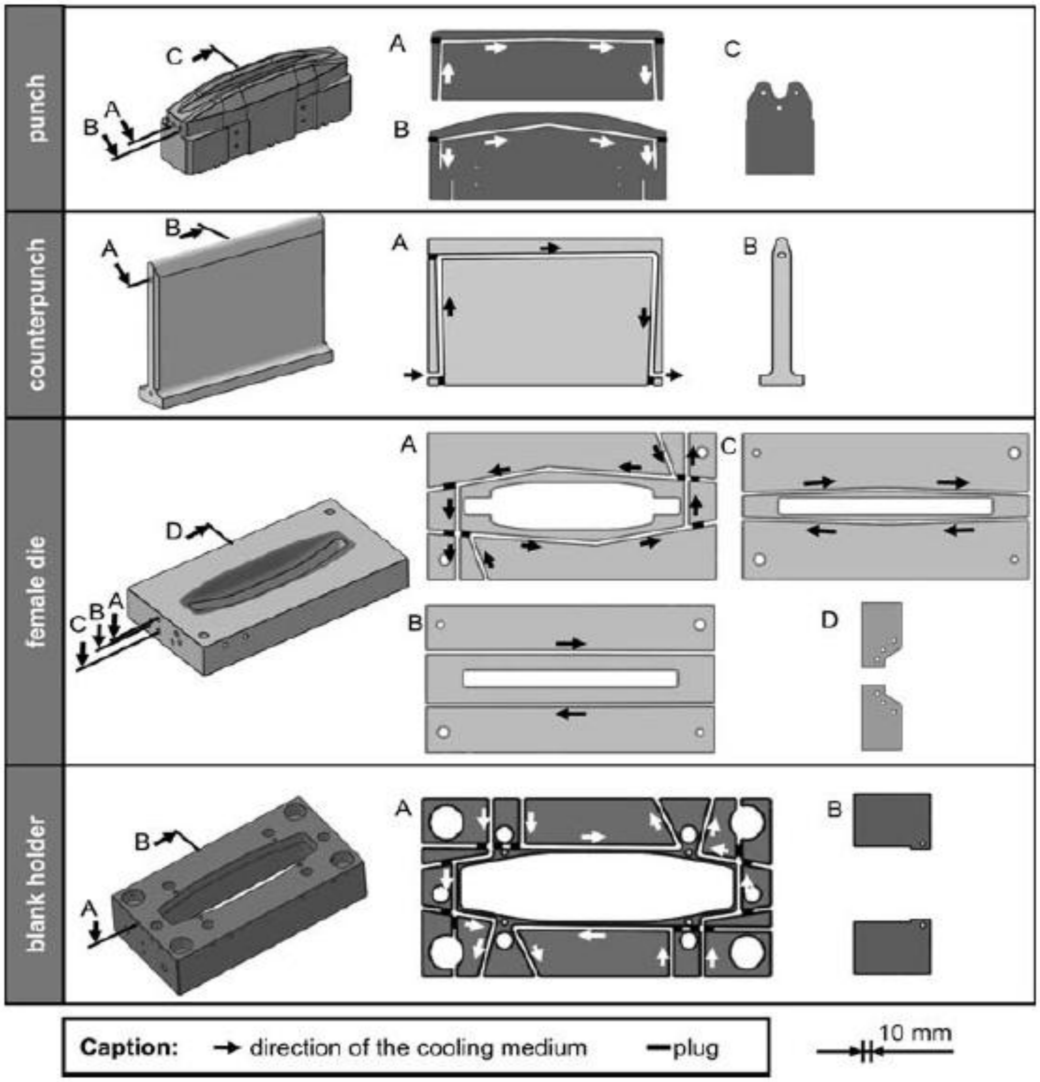

Figure 3.21 Optimized design of the cooling ducts for the tool components punch, female die, counterpunch and counter blank holder [STEI07]

3.3.4 Hot stamping dies with cast cooling channels

The method of casting cooling channels in the hot stamping dies is carried out by Kolleck et al. [KOLL05] at Institute of Tools and Forming, Graz University of Technology, Austria. This method improves the cooling performance of the tool and reduces the overall process cycle time.

The hot stamping tools with cooling ducts have to meet the following requirements

(i) Accuracy in achieving the desired cooling rate

(ii) Uniform temperature distribution on the surface of the tool (maximum deviation ± 5°C)

Conventional method of constructing cooling channels by drilling and milling has following disadvantages

(i) Complex cooling duct geometries cannot be made due to limited access

(ii) Higher amount of material removal leading to high cost factor

These disadvantages are overcome by casting cooling channels in the die block. The cooling channels can be accurately cast nearer to the tool surface to achieve the required cooling rate and temperature distribution.

The following steps are involved in building the tools

(i) Optimal or near perfect cooling ducts are fabricated

(ii) The fabricated cooling ducts are cast into grey cast iron or ductile graphite iron (High strength copper alloys can also be used as base material)

(iii) Using DMD (Direct Metal Deposition) technology, the tool surface is deposited with hard materials

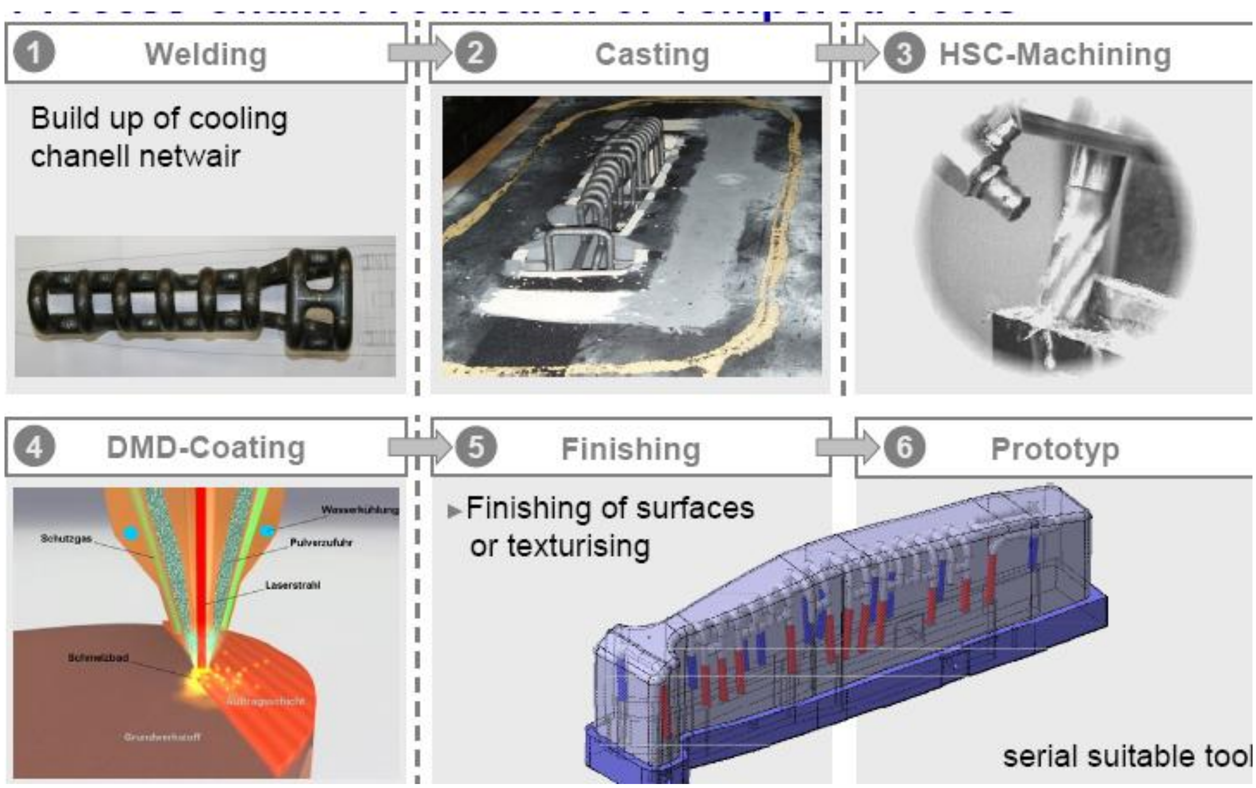

Figure 3.22 Steps involved in casting cooling ducts [KOLL05]

During the casting process, proper care must be taken in the following areas

(i) During the process of bonding between the molten metal and the tubes of cooling duct, air gaps may be formed affecting the heat transfer.

(ii) The tubes of cooling duct may distort during casting affecting flow of coolants

The flow analysis of the coolants in the cooling ducts was done using AVL Swift (Computational fluid dynamics software).

3.3.5 Tailor made tool materials for hot stamping [CASA08]

A correct compromise between tooling variables like initial tooling cost, durability, attainment of desired properties on the component and allowed productivity are key to increase the competitiveness of the hot stamping dies.

Introduction of extreme high thermal conductivity tool steels enabled the reduction of cycle time by reducing the holding time. Die materials like HTCS-117 (Ni, Cr and Mo die steel) reduced closed die cycle times from 10-15 s to 4-6 s. Now with the introduction of HTCS-130(High thermal conductivity tool steel originally developed for aluminum die casting), HTCS-150 and HTCS-170, the cycle time is further reduced to 2-3 s. These tool materials along with reduction in sheet transfer time from oven to die and increase in press speed are important parameters to optimize the hot stamping process.

Researchers are working on developing locally differentiated heat treatments in the hot stamped components to improve crash performance or to facilitate posterior cutting operations. One of the preferred way of achieving this is by having tools with varying thermal conductivities. The recently developed nanocasting technology can develop tools with complex cooling strategies at a reasonable price and any desired gradual or abrupt thermal conductivity variation in the range of 7-66 W/m K.

A study was conducted by [CASA08] on developing dies with gradually varying thermal conductivities from 60W/m K to 5-10 W/m K using nanocasting technology at Rovalma, Spain .Some welding materials used for repairing hot stamping dies and implementing dimensional changes are also studied by [CASA08] with different base material with different post heat treatments .Two high thermal conductivity welding alloys have been developed; one is available as TIG wire (HTCS-Rod) and the other is available as refurbished electrode (HTCS-RE). Post weld heat treatment severely increases heat conductivity, resilience and is always recommended.

3.4 Hard trimming of quenched parts and Characterization tests

The shearing and blanking of press hardened components is extremely demanding.HWS (cold work tool steel) steels are used for these applications provided they are robustly build, and cutting angles and clearances are very well adjusted. Trimming tool performance are affected by following factors.

(i) Slight blank movement in the moment of shearing/trimming

(ii) Local clearance maladjustment

(iii) Die cleanliness effect leading to material buildup near the cutting edge

(iv) Increase of blank thickness (poor scrap extraction or two blanks remaining under the press)

Small variation in the above factors increases the stress intensity at the cutting edge leading to premature failure in the form of chipping. Using HWS (Cold work tool steel), sheets with hardness in excess of 1800 MPa and press hardened components of more than 2mm thickness have been successfully sheared under close tolerances [CASA08].

3.5 Coatings for oxidation prevention

The coating of the blanks before heating is important for reducing oxidation and maintaining a good surface finish. 22MnB5 steel is generally supplied with Al-Si coating. ThyssenKrupp steel supplied 22MnB5 steel for the production of VW Passat with nanotechnology based coating(MBW-K ®1500 + X-TEC®) which gives short term corrosion protection and acts as lubricant during hot stamping [LENZ08].[MORI09] tested different lubricant oils supplied by Nihon Kohsakuyu Co., Ltd., Japan for their oxidation prevention properties during hot stamping process. These oils are generally used as lubricants for warm stamping of stainless steels and titanium sheets.

3.5.1 Effect of Coating

[WILS06, ALTA07a] explain that the heating of uncoated blanks must be carried out under protective atmosphere in order to avoid oxidation (scaling) and surface decarburization. [WILS06, ALTA07a] indicate that there is direct contact with atmospheric oxygen during the transfer of the blank from furnace to the press; oxidation occurs and forms an irregular and abrasive scale layer (iron oxides) on the blanks' surface. In this case, it is almost impossible to avoid some superficial decarburization (up to 60μm), which is harmful for final properties of the parts. Since the scale is characterized by extreme hardness, the hot stamping process may result in high die wear. Moreover, these parts should be shot-blasted or sand-blasted in order to remove scale layer. The shot-blasting is costly and can be harmful to geometrical tolerances of thin parts. This scaling during the hot stamping process can be largely avoided by means of surface coating.

3.5.2 Al-Si based coating

USIBOR 1500P supplied by Arcelor possesses an aluminum based pre-coating layer with a thickness between 23 and 32 μm . [WILS06, ALTA07a] describe that the Al-Si coating is transformed into a Fe-Al-Si layer during heating in the furnace. [WILS06] emphasizes that the heating rate must not exceed 12K/s since too rapid heating causes melting of the Al-Si coating before transformation into the heat resistant FE-Al-Si layer can happen.

Furthermore, [WILS06] recommends a proper dwell time in the furnace to guarantee a complete alloying of coating.

3.5.3 FE-Zn based coating

The boron steel is hot-dip galvanized. Due to diffusion processes during the austenitization phase, the Zn-layer transforms into a Zn-Fe layer [LAUM07]. Voestalpine developed a zinc based coating which offers scaling protection as well as cathodic corrosion protection according to [FADE06]. Hence, the corrosion protection is maintained even if the Zn-surface is damaged or interrupted for constructive reasons [LAUM07]. Furthermore, the lower layer hardness compared to Al-Fe coatings results in a lower die wear. Until now, galvanized 22MnB5 is applicable for indirect hot stamping only [STOP07].

3.5.4 X-Tec – nanotechnology based coating

ThyssenKrupp developed the X-Tec coating. [LENZ07, STOP07] describe the nanotechnology based painting, which is applied on the steel coil. According to [LENZ07] this coating protects the blank against corrosion and improves the lubrication between sheets and dies.

3.6 Other areas of importance [SCHA10]

To improve the crash performance and weight reduction in hot stamped components, tailor welded blanks are used. It has different steel grades with different thickness on the same blank. This allows adjusting the strength and elongation properties along the part leading to different deformation modes under crash situations. Variation in properties is also obtained by partial heating of the blank in the furnace and partial quenching of the part in hot stamping dies.

CHAPTER 4. FINITE ELEMENT SIMULATION OF HOT STAMPING PROCESS

It is important to predict the final properties of the hot stamped component early in the product development process. If precise predictions of the part geometry and micro structure can be obtained with numerical simulations, it is possible to create components with tailored properties and functionalities in different zones of the component. For example a B-pillar can be manufactured with softer material zones at its lower end. By allowing controlled buckling in this lower area, severe buckling at higher location with a possible penetration into passenger compartment can be prevented [AKER06].

4.1 Simulation of coupled thermo mechanical and microstructure evolution

Hot stamping simulation involves combined thermo mechanical and microstructure evolution simulation. [HEIN05] identified the following challenges in the finite element simulation of hot stamping process;

1, Temperature and strain rate dependent material parameters (thermal and mechanical)

2, Heat transfer between the blank and the die (depending on current contact conditions)

3, Coupled thermo-mechanical calculation

4, Evolution of microstructure of the material as a function of temperature, time and deformation.

The interaction between the mechanical field, thermal field and the microstructure evolution during hot stamping process is given in the schematic of Figure 4.1.

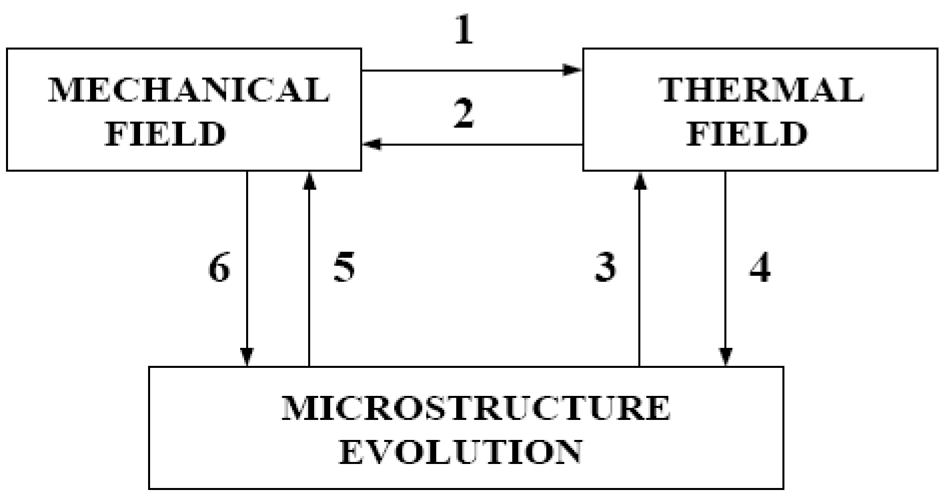

Figure 4.1 Interactions between the mechanical field, the thermal field and the microstructure evolution [OLDE08]

Table 4.1 Descriptions of interactions in Figure 4.1 [OLDE08]

No	Interaction Description
1a	Thermal boundary conditions are deformation dependent
1b	Heat generation due to plastic dissipation and friction (not accounted for in this work)
2	Thermal expansion
3a	Latent heat due to phase transformations
3b	Thermal material properties depend on microstructure evolution
4	Microstructure evolution depends on the temperature
5a	Mechanical properties depend on microstructure evolution
5b	Volume change due to phase transformations
5c	Transformation plasticity
5d	Memory of plastic strains during phase transformations
6	Phase transformations depend on stress and strain

The description of the different interaction parameters shown in the Figure 4.1 are given in Table 4.1.

The effects of some of the interaction parameters are important and some parameters can be neglected in the simulation. For example, the heat generation due to plastic deformation and friction can be neglected compared to the overall heat transfer between the blank and the tools [BERG99].

The parameter 1a, thermal boundary conditions based on deformation represents contact heat transfer coefficient between die and blank as function of pressure. The parameter 1b can be neglected in the simulation because of its negligible amount compared to the overall heat transfer between the blank and die. The parameter 2 and 5b can be included in the simulation by considering the variation of thermal dilatation value as a function of temperature. The parameter 3a can be included in the simulation by considering the variation of heat capacity of the material with respect to temperature. The parameters 3b and 5a represent the dependency of material parameters on the microstructure evolution based on a certain temperature history. There are two methods of considering these effects in the simulation. First, based on the information of volume fraction of different phases (austenite, ferrite, pearlite, bainite and martensite) and their properties, the overall material property can be calculated using mixture rules. Secondly, this effect can be considered directly by suitable material characterization experiments following appropriate temperature history. The second method is used widely. The parameter 4, can be calculated from the temperature history and equations like Koistinen-Marburger (for martensite evolution) [KOIS59].

The parameter 5C, transformation plasticity is an irreversible deformation that occurs when a material undergoes phase transformation under applied stress well below the yield strength of the material.. The parameter 5d is not considered in the finite element simulation.

4.2 Thermal and mechanical properties required for the high temperature forming simulation [ERIK02]

a) Flow stress data as function of strain, temperature and strain rate

Reliable flow stress data as function of temperature, strain and strain rate for both blank and die material is important for accurate numerical simulation. These datas are obtained by tensile test or compression test at high temperature.

b) Young's modulus as a function of temperature

Young's modulus is a description of the mechanical stiffness of the material. It is temperature dependent and it decreases at high temperatures.

c) Poisson's ratio as a function of temperature

Poisson's ratio relates the axial and lateral strain in uniaxial compression or tension.

d) Thermal dilatation due to thermal expansion and phase transformation

Thermal expansion and volume change due to transformation of austenite to martensite under controlled cooling conditions evaluated using dilatation tests are required for the numerical simulation.

e) Thermal conductivity as a function of temperature

Thermal conductivity defines the ability of a material to transfer heat. This property is phase and material dependent.

f) Heat capacity as a function of temperature

Heat capacity of a material represents amount of energy required to produce a unit temperature rise. This property is phase and temperature dependent. The heat capacity function includes the effects of the latent heat released during the transformation from austenite to martensite.

g) Heat transfer coefficient between die and sheet material

Heat transfer coefficient between die and sheet material during the hot stamping process changes as a function of distance until the die actually touches the sheet material and as a function of pressure during deformation process.

h) Transformation induced plasticity

During phase transformations the material undergoes plastic deformation even if the applied stress is lower than the yield stress. It occurs by two mechanisms; 1) the volume difference between the phases generates internal stresses large enough to cause plastic deformation in the weaker phase(Greenwood-Johnson mechanism).The formation of the new phase (martensite in this case) occurs in a preferred orientation which influences the global shape of the material (Magee mechanism).

4.3 Constitutive model for hot stamping by [AKER06a,07]

A thermo-elastic-plastic constitutive model based on the Von Mises yield criterion with associated plastic flow was developed by [AKER06a, AKER07] from Lulea University of Technology, Sweden. This model includes the effect of austenite decomposition and transformation induced plasticity. This model is suitable for FE simulation using the explicit method.

In this model,the total strain increment during each time step of hot stamping simulation is given by the following equation[AKER07]

$$\Delta\varepsilon_{ij} = \Delta\varepsilon_{ij}^{\mathrm{e}} + \Delta\varepsilon_{ij}^{\mathrm{th}} + \Delta\varepsilon_{ij}^{\mathrm{tr}} + \Delta\varepsilon_{ij}^{\mathrm{p}} \quad \text{………………………..(20.3)}$$

where $\Delta\varepsilon^{e}_{ij}$ is the elastic strain increment, $\Delta\varepsilon^{th}_{ij}$ is the thermal strain increment, $\Delta\varepsilon^{tr}_{ij}$ is the isotropic transformation strain increment and $\Delta\varepsilon^{p}_{ij}$ is the plastic strain increment.

Based on the work from [AKER06, 06a] ,material model *MAT_244 is developed and implemented in LS-Dyna for hot stamping application. This model is quite computing intense. Using this model final phase and hardness values at different part of the geometry can be predicted.

4.4 Case study 1

4.4.1 Simulation of hat shape using DEFORM

An example part and die geometry was chosen from [AKER06a].The die geometry used for simulation is given in Figure 4.2.

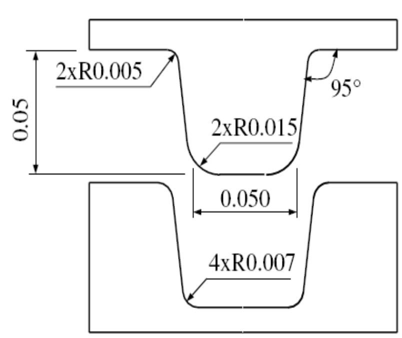

Figure 4.2 Die geometry for hat shape, All dimensions are in m [AKER06a]

During the experiment conducted by [AKER05], the following parameters were measured.

1, Forming force Vs time

2, Temperature at the edge of steel strip as shown in Figure 4.3.

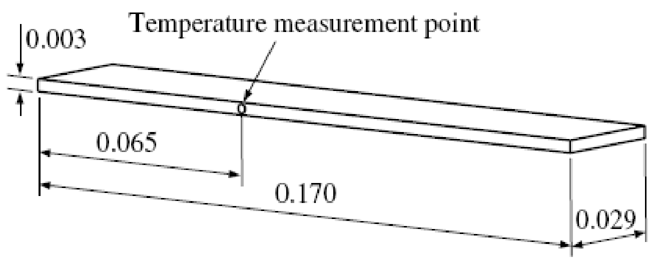

Figure 4.3 Steel strip used for the experiment and the temperature measurement point, dimensions are in m [AKER06a]

The 3D simulation was conducted using DEFORM with following input parameters.

Material data

Sheet material: 22MnB5

Die material: AISI-H13

Flow stress data for 22MnB5-[NUMI08]

Emissivity of 22MnB5=0.6

Thermal conductivity of 22MnB5=32 W/m K (constant)

Specific heat capacity of 22MnB5=650J/kg K (constant)

Material properties for AISI-H13 are available in DEFORM data base.

Process parameters

Velocity of punch=10mm/s

Duration of forming process=5s

Initial temperature of tool=26°C

Temperature of the environment=30°C

Heat transfer coefficient between sheet and die=6500 W/m2K (constant)

Coefficient of friction=0.3

Simulation setup

The sheet material type is chosen as plastic and meshed with 8-node brick elements and the die is meshed with 4-node tetrahedral element. Only one quarter of the geometry is modeled due to planar symmetry. The initial simulation setup is given in Figure 4.4.

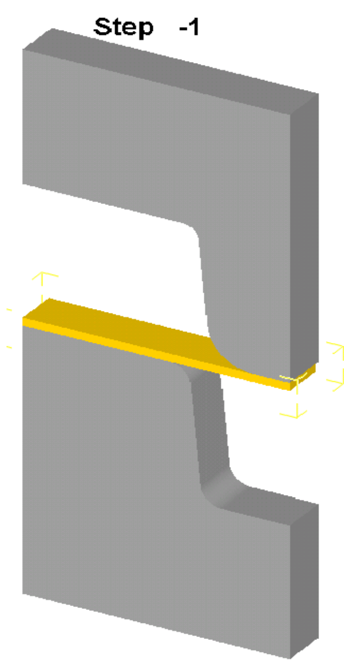

Figure 4.4 Initial simulation setup in DEFORM 3D

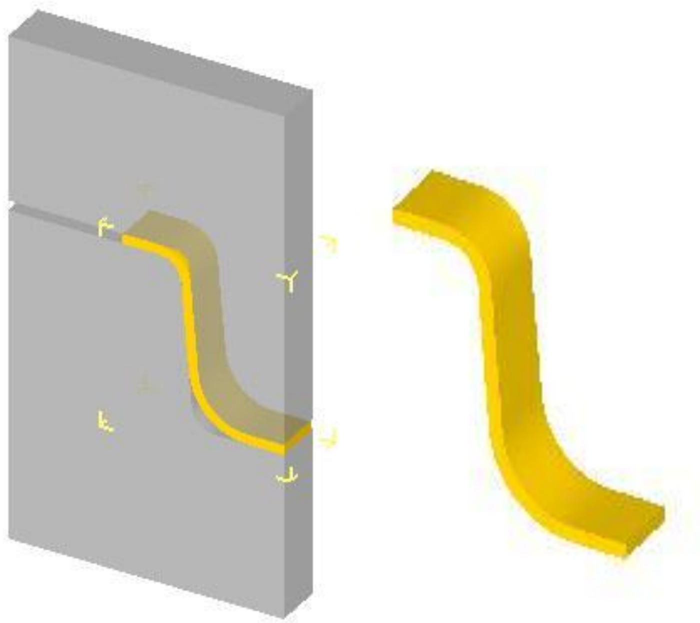

Figure 4.5 Final simulation step (left) and formed part (right)

Simulation results

The results of the simulation are given in Figure 4.6 and Figure 4.7.

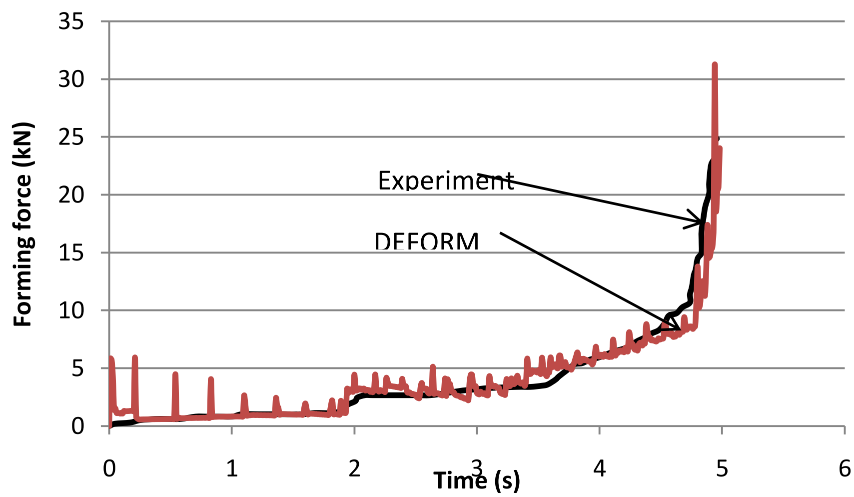

Figure 4.6 Comparison of experimental and calculated forming force Vs time

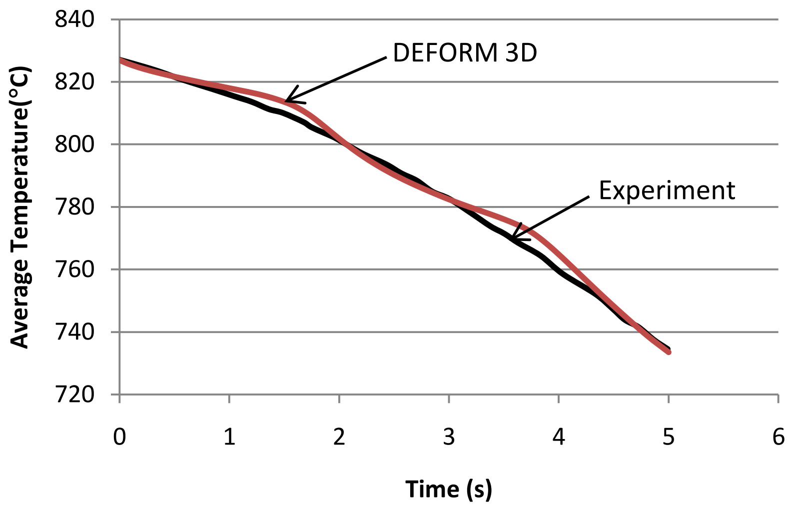

Figure 4.7 Comparison of experimental and calculated temperature versus time

The temperature was measured at the edge of the steel strip at a given point as shown in Figure 4.3. In the simulation an average temperature is calculated at 3 nodes at the specified location. The calculated forming force and temperature have good agreement with experimental results.

Notes

Initially 2D simulation of the part was conducted with the assumption of plane strain condition. In the 2D simulation, whenever the punch touches the temperature measurement point, there is a sharp decrease in temperature. The reason was found to be higher value of the heat transfer coefficient between tool and the blank as given in the reference. However, the same value is used for the 3D simulation to compare DEFORM results with the reference. The flow stress data for 22MnB5 in this simulation is chosen from Numisheet-2008 Benchmark problem-3.Simulation by considering the blank as elasto-plastic material runs successfully.

4.5 Case study-2

4.5.1 Simulation of Benchmark problem-3, Numisheet-2008

AUDI proposed virtual modeling of hot stamping process of a B-pillar reinforcement, Figure 4.8. The objective is to predict sheet thickness distribution, necking failure and the local degree of hardness in the final part.

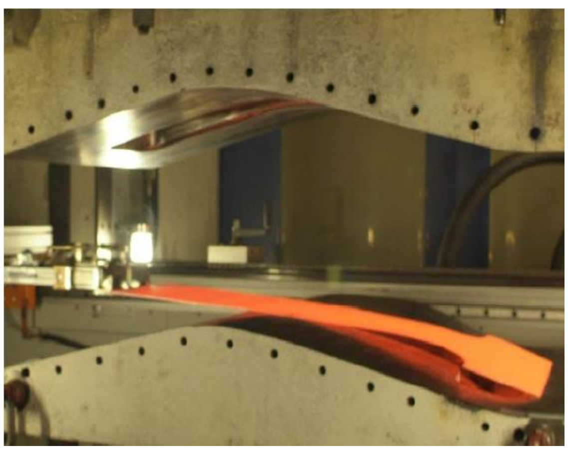

Figure 4.8 Actual setup of the proposed problem [ARTH09]

The process steps involve

1, Heating of the blank to 940°C.

2, Transport from the oven into the tool (6.5s)

3, Forming of part geometry in the tool (1.6s)

-Temperature of the blank at the beginning of the die movement: 810°C

-Temperature of the tools: 75°C

-Travel curve for the die (die stroke vs time)

Time(s)	Die stroke(mm)
0	0
0.05	19.6
0.17	65.4
0.29	110.9
0.41	156.1
0.53	201.5
0.65	239
0.77	260.1
0.89	280.6
1.01	294.4
1.13	306
1.25	316.5
1.37	322.4
1.49	329.1
1.61	329.8

-Punch is fixed

4, Quenching time in the tool (20s)

-Double sided tool contact

The blank material used is 22MnB5+AlSi of thickness 1.95mm.The mechanical and thermal properties of 22MnB5 as given by AUDI is shown in Table 4.2.

.

Table 4.2 Mechanical and thermal material properties of 22MnB5 (AUDI)[NUMI08]

Young's modulus	E	100,000 MPa
Poisson's ratio	ν	0.3
Coefficient of thermal expansion	α	1.3 x 10-5 (1/K)
Heat conductivity	K	32 W/mK
Heat transfer coefficient	hair htool	160 W/m2K p=0 MPa,1300 W/ m2K p=20 MPa,4000 W/m2K p=35MPa,4500 W/ m2K
Friction	μ	0.4

The flow stress data of 22MnB5 as a function of temperature, strain and strain rate from University of Erlangen, Germany is given as input.

Simulation setup

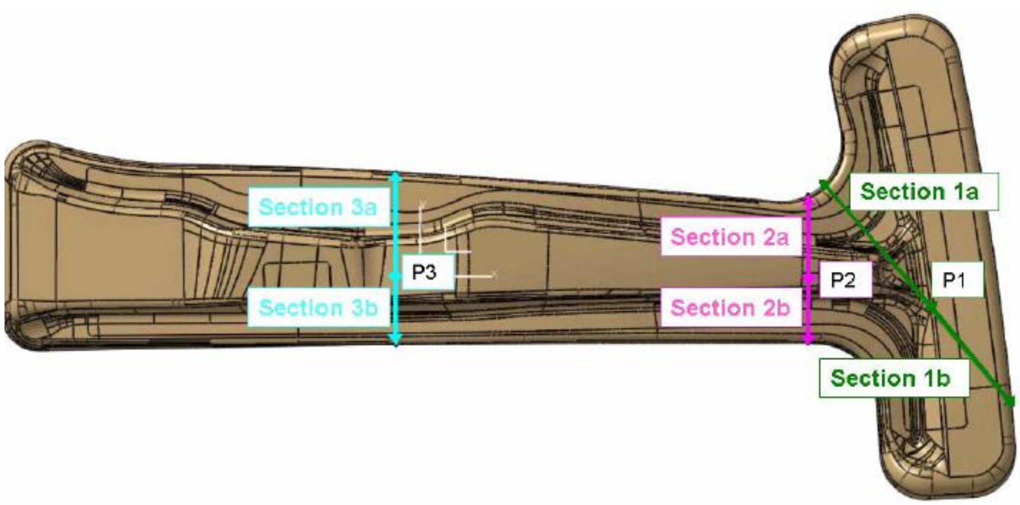

Figure 4.9 Sections to be analyzed as given in Numisheet2008, Benchmark problem-3

From the given 3D CAD files, section 3 is obtained using SOLIDWORKS for the 2D simulation in DEFORM.

The entire hot stamping process is simulated by considering tools as rigid and the blank as elasto-plastic. During forming process, two simulations are conducted by assuming (i) constant die temperature as given in the problem statement and (ii) calculating heat transfer in dies.

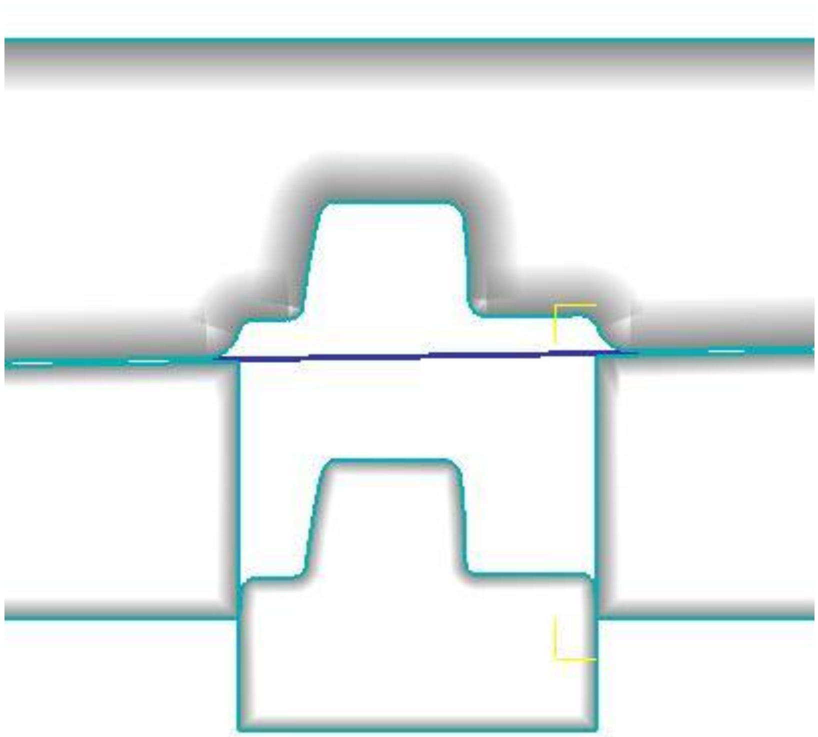

Figure 4.10 Initial forming simulation setup for Section-3 of B-Pillar

Simulation of hot stamping process

(i) Heating the blank (Austenitisation)

An initial temperature condition of 20°C is considered for the blank which is heated to 940°C. FE model resulted in a thickness change from 1.95mm to 1.98mm due to thermal expansion.

(ii) Transport from oven to the tool

For this process, the process time 6.5 s is given. Hence, the convective heat transfer coefficient between air and the blank is varied to reach a minimum blank temperature of 810°C. The convection coefficient is found to be 50 W/m^2 K. The default value in DEFORM is 20 W/m^2 K.

(iii) Blank resting on the die

This is the time interval from starting of die downward stroke to the time at which it touches the blank. The duration is 0.53 s. During this process, section-3 does not touch the tools and the heat transfer is only with environment. The temperature distribution of the blank at the end of this process is in the range 780-802°C.

(iv) Forming process

At the beginning of the forming step, the clearance between top die and blank holder is kept as 1.95+0.4 mm. In actual hot stamping process both top die and blank holder move down and the punch remains stationary. In this simulation punch is moving whereas top die and blank holder remain stationary. Once the load reaches 35MPa (5740 N),the forming process stops. This simulation is conducted with constant die temperature and varying die temperature. The part geometry and temperature distribution at the end of the forming stroke with constant die temperature is given in Figure 4.11. The part geometry and temperature distribution at the end of the forming stroke with varying die temperature is given in Figure 4.12.

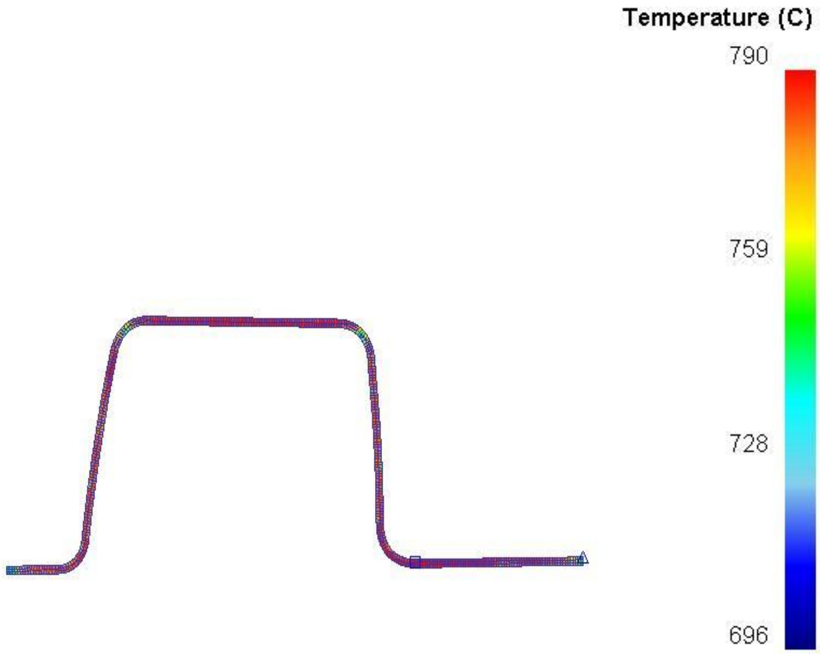

Figure 4.11 Part geometry and temperature distribution at the end of the forming process with constant die temperature

Figure 4.12 Part geometry and temperature distribution at the end of the forming process with varying die temperature

The final temperature of the part at the end of the forming stroke in both simulation cases is in the range 696 - 790°C. Hence, forming process can be simulated with constant die temperature to get results with reasonable accuracy.

Notes

The given stroke versus time data (from 0.65s to 1.61s) is fitted to second order polynomial. By taking first derivative of the polynomial velocity is calculated. This velocity versus time data is given as input for punch movement.

Considering blank as elastic-plastic model resulted in difficulties in convergence of solution in DEFORM. The reasons were found to be extrapolation error of flow stress data at higher strain rates. This was taken care by assuming constant flow stress data at higher strain rates.

(v) Quenching process

During this process a constant closing pressure of 35MPa is considered between tools and the formed part. The duration of this process is 20s.The temperature distribution at the end of the quenching process is given in Figure 4.13.

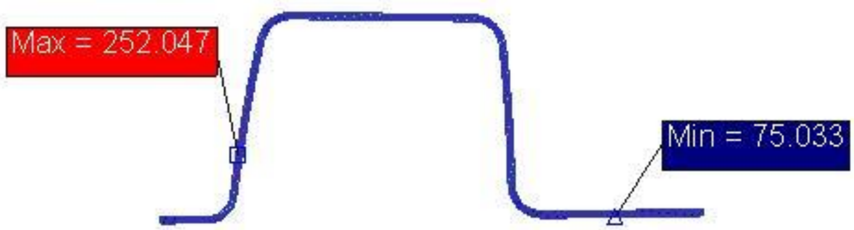

Figure 4.13 Maximum and minimum temperature at the end of the quenching process with constant die temperature

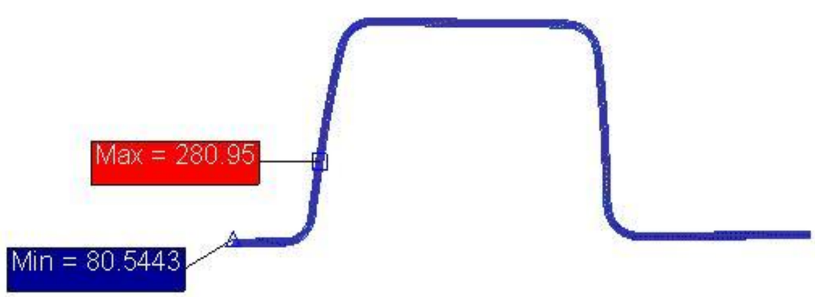

Figure 4.14 Maximum and minimum temperature at the end of the quenching process with varying die temperature

(vi) Air cooling

To get the final thickness distribution of the part, heat transfer simulation is conducted until the part temperature reaches to 20°C.The obtained thickness distribution for section 3a with constant and varying die temperature are compared with experimental results.

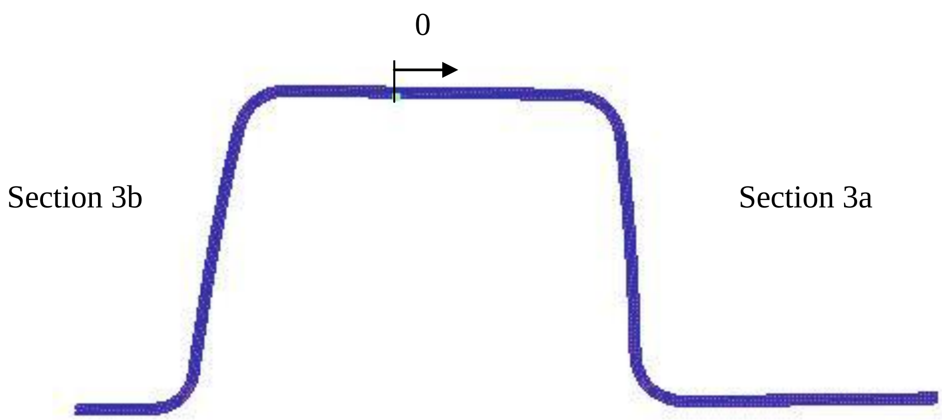

Figure 4.15 Final part showing the origin point for thickness distribution calculation

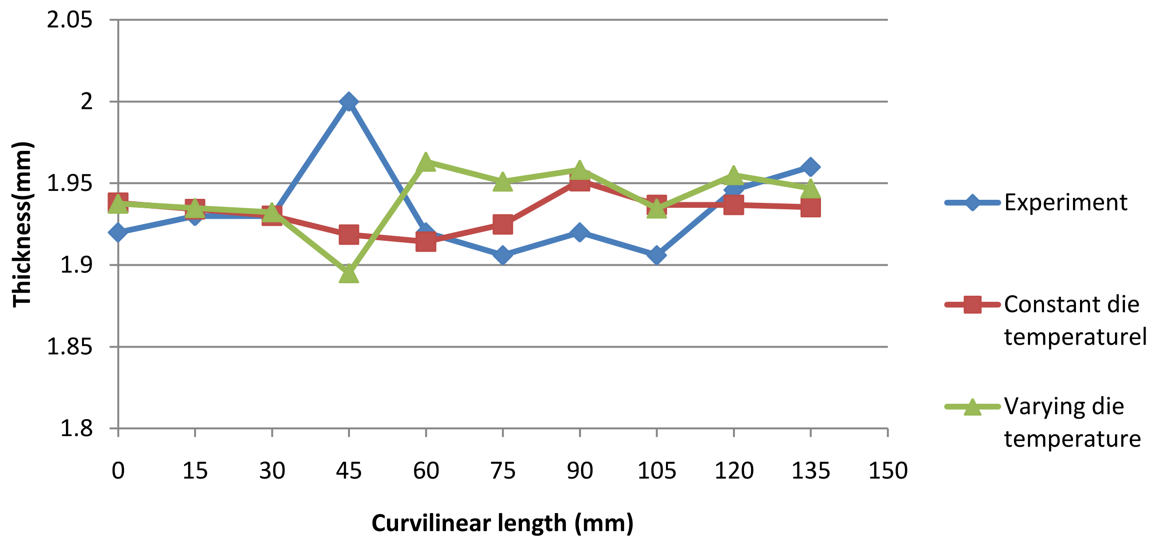

Figure 4.16 Comparison of thickness distribution in section 3a

At curvilinear length=45mm, thickening of the part is observed in the experimental case whereas DEFORM results showed thinning.

CHAPTER 5. FUTURE WORK

(i) Material data for 22MnB5 steel has to be updated for higher strain rates.

(ii) A methodology for hot stamping tool design has to be developed

(iii) A methodology for cooling channel design and optimization has to be developed

(iv) Simulation of trimming of the final part and tool wear study has to be conducted

List of References

[AKER05] Akerstrom,P.,Wikman,B.,Oldenburg,M.,”Material parameter estimation for boron steel from simultaneous cooling and compression experiments”Modelling and simulation in material science and engineering 13,1291-1308,2005

[AKER06] Akerstrom, P., Oldenburg, M.,”Austenite decomposition during press hardening of boron steel”, Journal of material processing technology 174,399-406,2006

[AKER06a] Paul Akerstrom ,”Modeling and simulation of hot stamping”, Doctoralthesis,Department of applied physics and mechanical engineering, Lulea university of Technology, Sweden, 2006

[AKER07] Akerstrom, P.,Bergman,G., Oldenburg, M., ”Numerical implementation of a constitutive model for simulation of hot stamping”, Modeling and simulation in material science and engineering 15,105-119,2007

[ALTA07a] Altan, T.; Yadav, A., ”Hot Stamping Boron-alloyed Steels for Automotive Parts – Part II” ERC/NSM, Ohio State University, Stamping Journal, Jan. 2007

[AMBI10] Ambikapathy, N., Altan, T., ”Hot stamping technology-Fundamentals and applications”, Center for precision forming, The Ohio State University, Report No.CPF-5.5/10/01

[ARTH09] Arthur B.Shapiro, ”Using LS-Dyna for hot stamping”,7th European LS-Dyna conference,2009

[ASPA08] Aspacher , J., ”Forming hardening concepts”, 1st International conference on hot sheet metal forming of high performance steel,Kassel,Germany,77-81

[BERG99] Greger Bergman,” Modeling and simulation of simultaneous forming and quenching”, Division of computer aided design, Department of mechanical engineering, Lulea university of Technology, Sweden,1999

[BERG08] Berglund, Amundsson, K., Hellgren, L, O.,”Hot stamped components with “soft zones” for improved crashworthiness simulation and validation of product performance”, Gestamp R & D, Luleå, Sweden, International Deep Drawing Research Group Proceedings, Olofström, Sweden, June 2008

[BERG08a] Berglund. G., ”The history of hardening of boron steel in northern Sweden” ,1st International conference on hot sheet metal forming of high performance steel,Kassel,Germany,175-177

[BEHR08] Beherens,B.,Olle,P.,Schaffner,C.,“Process simulation of hotstamping in consideration of transformation induced stresses”, Numisheet2008, Interlaken, Switzerland,2008

[BHAD92] Bhadeshia, B.K.D.H., ” Bainite in steels”, Number 504,The institute of materials, 1992 0-901462-95-0

[BRYA07] Bryan Macek , ”Developing a deep drawn hot stamped fuel tank guard”, Bentler Automotive, Great designs in steel seminar,2007

[CASA08] Begona Casas, David latre, Noemi Rodriguez, Isaac Valls," Tailor made tool materials for the present and upcoming tooling solutions in hot sheet metal forming", Steel grips 6 (2008) Suppl. CHS2

[ENGE06] H. Engels, O. Schalmin, C. Müller-Bollenhagen ,"Controlling and Monitoring of the Hot-Stamping Process of Boron-Alloyed Heat-Treated Steels", The International Conference "New Development in Sheet Metal Forming Technology", pp. 135~150, Stuttgart / Germany,2006

[ERIK02] Eriksson,M., Oldenburg,M., Somani,M,C., Karjalainen,L,P., "Testing and evaluation of material data for analysis of forming and hardening of boron steel components", Modeling and simulation in material science and engineering,277-294,2002

[FADE06] Faderl, J.; Radlmayr, K.M., "Ultraform und ultraform_PHS – Innovation made by voestaplina" Voestapline Stahl GmbH, 1. Erlangener Workshop Warmblechumformung 2007, Bamberg, Meisenbach 2006

[GEIG08] Geiger, M., Merklein, M., Lechler, J.,"Determination of tribological conditions within hot stamping", German Academic Society for Production Engineering, 2008

[HEIN05] Hein, P.,"A global approach of the finite element simulation of hot stamping", Arcelor Flat Carbon Steel, Automotive Research Center, Montataire, France, Advanced Materials Research Vol.6-8,2005,pp 763-770

[HOFF07] Hoffmann, H., So, H., Steinbeiss, H., “Design of hot stamping tools with cooling system”, Annals of the CIRP, Vol 56/1,2007

[KARB09] Hossein Karbasian, and A. Erman Tekkaya, ”A review on hot stamping”, submitted to Journal of material processing technology,2009

[KIRK83] Kirkaldy . J . S., Venugopalan . D.,”Prediction of microstructure and hardenability in low alloy steels,in: A.R. Marder, J.I.Goldstein (Eds), International conference on phase transformations in ferrous alloys, October 1983,Philadelphia,125-148

[KOIS59] Koistinen. D.P., Marburger. R.E. ,”A general equation prescribing the extent of the austenite- martensite transformations in pure iron-carbon alloys and plain carbon steels, Acta Metall.7 ,59-60,1959

[KOLL05] Kolleck, R., Pfanner, S., Warnke, E.-P., Ganter, R.,“ New concept for tempering sheet metal forming Tools”

[KOLL09] Kolleck, R., Veit, R., Merklein, M., Lechler, J., Geiger,M.,”Investigation on induction heating for hot stamping of boron alloyed steels ”,CIRP Annals,275-278,2009

[LARS08] Lars, P., Altan, T.,”Hot Stamping of Ultra High Strength Steel”, Report No.CPF-5.5/08/01,Center for Precision Forming, The Ohio State University, March 2008

[LAUM07] Laumann, T.; Pfestorf, M., ”Potential verzinkter Warmumformteile für den Einsatz in der Rohkarosserie” BMW Group, 2. Erlangener Workshop Warmblechumformung 2007, Bamberg, Meisenbach 2007

[LECH09] Jurgen Lechler,”Pressharten von Bor-Manganstahlen“, Fertigunstechnik-Erlangen,200,ISBN 978-3-87525-286-6,2009

[LENZ07] Lenze, F.-J.; Bian, J.; Sikora, S., ”Einsatz pressgehärteter Stähle im Karosseriebau: Stand und Trends der Entwicklung” ThyssenKrupp Steel AG, 2. Erlangener Workshop Warmblechumformung 2007, Bamberg, Meisenbach 2007

[LENZ08] Lenze, F, J., Banik, J., Sikora, S.,”Applications of hot formed parts for body in white”, ThyssenKrupp Steel, Dortmund, Germany, International Deep Drawing Research Group Proceedings, Olofström, Sweden, June 2008

[MAYN78] Ph.Maynier, B.Jungmann, J.Dollet, ”Creusot-loire system for the prediction of mechanical properties of low alloy steel products”, in: D.V.Doane, J.S.Kirkaldy(Eds),Hardenability concepts with applications to steel,AIME,Warrendale,PA,1978,P.518

[MERK06a] Merklein, M., Lechler, M., Geiger, M.,” Characterization of the Flow Properties of the Quenchable Ultra High Strength Steel 22MnB5”, Institute of Mechanical Engineering, University of Erlangen-Nuremberg, Annals of CIRP Vol.55/1/2006

[MERK06b] Merklein, M., Lechler, M.,” Investigation of the thermo-mechanical properties of hot stamping steels”,Journal of materials processing technology 177,452-455,2006

[MERK08a] Merklein, M., Lechler, J., Stoehr,T., ”Characterization of tribological and thermal properties of metallic coatings for hot stamping boron manganese steels”, Proceedings of the 7th International conference ” THE ”, Coatings in manufacturing engineering,219-228,1-3 October,2008

[MORI05] Mori, K., Maki, S., Tanaka, Y.,” Warm and Hot Stamping of Ultra High Tensile Strength Steel Sheets Using Resistance Heating”, Department of Production Systems Engineering, Toyohashi, Japan, Annals of CIRP Vol.54/1/2005

[MORI09] Mori, K., Ito, D.,”Prevention of oxidation in hot stamping of quenchable steel sheet by oxidation preventive oil”, CIRP Annals,267-270,2009

[NICH08] Nicholson, R.,”Hydraulic presses for hot stamping”, Stamping Journal, October, 2008

[NUMI08] Numisheet 2008,The Numisheet Benchmark study,Benchmark problem BM03,Interlaken,Switzerland,September,2008

[OLDE08] Oldenburg, M., Åkerström, P., Bergman, G., Salomonsson, P., ”Modeling of microstructure and material response in the press hardening process”, International Deep Drawing Research Group Proceedings, Olofström, Sweden, June 2008

[PAAR07] Paar, U.; Valls, I., ”Werkzeugstähle und Strategie für Warmumformung und Hartbeschneiden” Volkswagen AG, 2. Erlangener Workshop Warmblechumformung 2007, Bamberg, Meisenbach 2007

[SCHA10] Schaeper, E., Wilsius, J., “Prediction of the formability of hot stamped parts”, International conference on New developments in sheet metal forming”,Stuttgart,Germany,May2010,pp305-319.

[SIEB55] Siebel E, Beisswa¨nger H (1955) Tiefziehen, Mu¨nchen-Hanser

[SHVE64] Shvets, I, T., “Contact heat transfer between plane metal surfaces”, Int.Chem.Eng.Vol.4, No.4, Page.621, 1964

[STEI07] Steinbeiss, H., So, H., Michelitsch, T., Hoffmann, H., ”Method for optimizing the cooling design of hot stamping tools”, Production Engineering Research and Development,Vol1,No.2,149-155,2007

[STOP07] Stopp, R.; Schaller, L.; Lamprecht, K.; Keupp, E.; Deinzer, G., ”Warmblechumformen in der Automobil-Serienfertigung – Status, Trends, Potenziale” AUDI AG, 2. Erlangener Workshop Warmblechumformung 2007, Bamberg, Meisenbach 2007

[YANA09] Yanagida, A., Azushima, A.,” Evaluation of coefficients of friction for hot stamping by newly developed tribosimulator”, International deep drawing research group, IDDRG 2009 International Conference, Golden, CO, USA, 2009

[WILS06] Wilsius, J.; Hein, P.; Kefferstein, R., ”Status and future trends of hot stamping of USIBOR 1500 P” Arcelor Research Automotive Applications, 1. Erlangener Workshop Warmblechumformung 2006, Bamberg, Meisenbach 2006